Zoological Journal of the Linnean Society, 2025, **205**(**4**), zlaf150
https://doi.org/10.1093/zoolinnean/zlaf150

OXFORD

Original Article

Nasal turbinals and laminae homologies in pangolins: insights from developments

Kai Ito[1,2,*], Ryo Kodera[2], Mugino O. Kubo[1], Noriyuki Kuroda[2], Quentin Martinez[3]

[1]Department of Natural Environmental Studies, Graduate School of Frontier Sciences, The University of Tokyo, Kashiwa, Chiba 277-8563, Japan
[2]Department of Anatomy, School of Dental Medicine, Tsurumi University, Yokohama 230-8501, Kanagawa, Japan
[3]Staatliches Museum für Naturkunde Stuttgart, Stuttgart DE-70191, Germany

[*]Corresponding author. Department of Natural Environmental Studies, Graduate School of Frontier Sciences, The University of Tokyo, 5-1-5 Kashiwanoha, Kashiwa, Chiba 277-8563, Japan.
E-mail: kai-ito@g.ecc.u-tokyo.ac.jp

ABSTRACT

The mammalian nasal cavity houses complex turbinals and laminae that conserve heat and moisture and mediate olfaction. Despite renewed interest driven by CT technology, some mammals remain scarcely studied, especially from developmental perspectives. This is true for pangolins, hypothesized to possess unique turbinals due to their elongated rostrum and possible olfactory adaptations for a specialized diet. Their turbinal complexity makes it difficult to establish hypotheses of homology with other mammals. Foetal anatomy and ontogenetic changes in the nasal capsule, therefore, provide key insights for assessing turbinal homology. Using diceCT, we reconstructed the foetal nasal capsules of *Manis pentadactyla* and *M. javanica*, and examined adults representing seven pangolin species, to clarify homology. By mapping turbinal and lamina traits on to a molecular phylogeny, we propose an evolutionary scenario for the morphology. Maxilloturbinals differ between Asian pangolins (double-scrolled folds) and African pangolins (a double scroll with a small caudal branch). Ethmoturbinal complexity also varies: in all pangolins, ethmoturbinal I comprises rostral (pars anterior) and caudal (pars posterior) portions, with lineage-specific degrees of subsequent fusion. These observations support two possible evolutionary pathways for the ethmoturbinal I: (i) complete separation into distinct pars; (ii) initial separation followed by secondary fusion in some lineages.

Keywords: Pholidota, evo-devo, skull, microCT (μCT), homology, turbinal, olfaction

INTRODUCTION

Bony or cartilaginous plate-like structures called turbinals and laminae occupy the mammalian nasal cavity (e.g. Moore 1981, Smith *et al.* 2015, 2021a, Martinez *et al.* 2024a). Turbinals increase its surface area through their complex branching and scrolling (e.g. Parker 1874, 1885, Martineau-Doizé *et al.* 1992, Smith *et al.* 2021a, b, Martinez *et al.* 2024a). Their surfaces bear goblet cells, olfactory receptors, and capillaries that warm inhaled air, retain humidity, and support olfactory cells (e.g. Negus 1958, Hillenius 1992, Smith *et al.* 2021b, Martinez *et al.* 2024a). The number and the surface area of these turbinals vary greatly among species due to ecological adaptations and phylogenetic inertia (Paulli 1900a, b, c, Van Valkenburgh*et al.* 2011, 2014, Green *et al.* 2012, Macrini 2012, Ruf 2014, Martinez *et al.* 2018, 2020, 2024a, b).

The nasal cavity contains turbinals known as the marginoturbinal, atrioturbinal, nasoturbinal, maxilloturbinal, ethmoturbinal, epiturbinal, frontoturbinal, and interturbinal (Maier 1993a,b). The marginoturbinal lies nearest to the external naris, followed by the atrioturbinal; neither ossifies (Maier 1980, 2000, 2020, Zeller 1987, Göbbel 2000, Maier and Ruf 2014, Smith *et al.* 2015). The nasoturbinal is a dorsal, elongated element linked to the nasal bone, extending rostrocaudally (Moore, 1981). The maxilloturbinal lies anteroventrally and exhibits complex branching in many mammals (Negus 1958, Van Valkenburgh *et al.* 2004, 2014b, Maier and Ruf 2014, Smith *et al.* 2015, Martinez *et al.* 2018, 2023a, 2024a, b, Wright *et al.* 2024).

Multiple ethmoturbinals occupy the ethmoturbinal recess, a caudal region of the nasal cavity, fusing with the ethmoid bone (Van Gilse 1927, Smith *et al.* 2015). Ethmoturbinal I is the largest, splitting into anterior and posterior portions (Voit 1909, Maier 1993a, Ruf 2020). Several small laminae extend from each ethmoturbinal and are referred to as epiturbinals (Maier 1993b, Smith and Rossie 2008).

The frontoturbinal recess, a dorsal space in the nasal cavity, contains multiple frontoturbinals (Maier 1993a, b, Rossie 2006). Several interturbinals also occur in both the ethmoturbinal and

Received 19 April 2025; revised 7 September 2025; accepted 16 September 2025

frontoturbinal recesses, but protrude less prominently than other major turbinals (Maier 1993a, b).

In addition to the turbinals, the nasal cavity houses three laminae: lamina semicircularis, lamina horizontalis, and lamina transversalis. The lamina horizontalis (frontomaxillary septum) divides the lateral recess into the frontoturbinal and maxillary recesses (Rossie 2006, Smith and Rossie 2008, Maier and Ruf 2014, Ruf 2014).

The nasal capsule, representing the foetal nasal cavity, develops at the rostral end of the chondrocranium (Moore 1981, Kaucka *et al.* 2018). Cartilage that forms certain turbinals and laminae projects within it (Dieulafe and Loeb 1906, Maier 1993a, Ruf 2020) (Fig. 1). Morphogenesis proceeds via three mesenchymal condensations: the parietotectal cartilage (pars anterior), the paranasal cartilage (pars lateralis or intermedia), and the orbitonasal lamina (pars posterior) (de Beer 1937, Reinbach 1952b, Moore 1981, Zeller 1987, Rossie 2006, Smith and Rossie 2006, 2008, Van Valkenburgh *et al.* 2014a, b, Martinez *et al.* 2024a). The nasal capsule is enclosed by exocranial facial bones (palatine, maxilla, and nasal) and is integrated into the adult nasal structure. Turbinals and laminae grow increasingly complex, branching and scrolling (Maier and Ruf 2014). Because the nasal capsule undergoes complex morphological transformations during ontogeny, observing its form at various developmental stages is essential for reliable structural identification. Such an ontogenetic approach also facilitates robust assessment of homologies among phylogenetically distant taxa.

The CT technology has advanced turbinal homology research, especially for large or rare mammals where histology is impractical. However, some clades, such as pangolins (Pholidota), remain poorly studied. Pangolins, covered in thick keratinous scales, were long considered close relatives of armadillos (Cingulata) due to morphological and ecological similarities (Reinbach 1952b, Wilson and Mittermeier 2011). Linnaeus (1758) classified pangolins

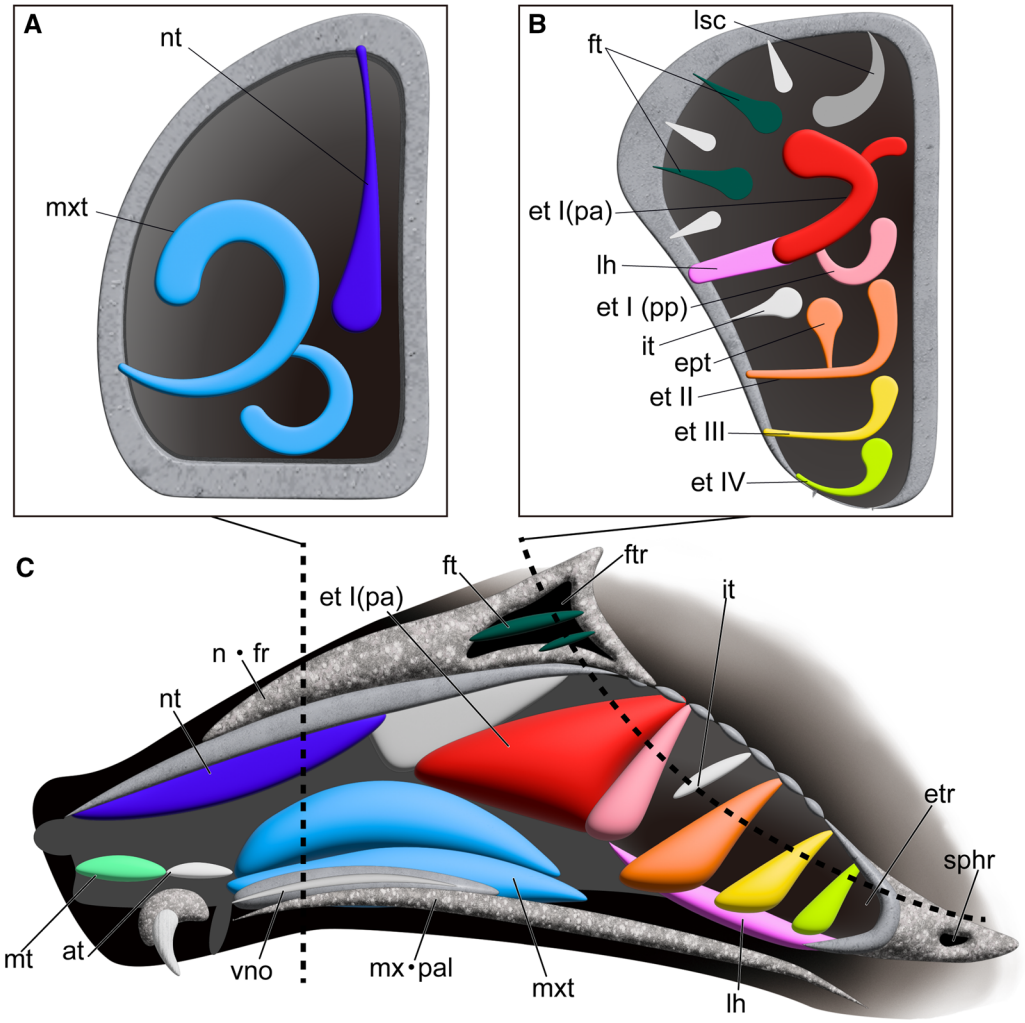

Figure 1. Generalized schematic mammalian nasal capsule. A, coronal section through the rostral part of the nasal capsule; B, coronal section through the caudal part of the nasal capsule, modified from Maier (1993b); C, medial view of parasagittal section modified from Maier (1993a) and Maier and Ruf (2014). All facial exocranial bones except the maxilla and palatine are removed, and the lamina semicircularis is partly excised to expose the frontoturbinals. Dashed lines indicate each coronal section. Abbreviations: at, atrioturbinal; ept, epiturbinal; et I (pa), ethmoturbinal I pars anterior; et I (pp), ethmoturbinal I pars posterior; et II–IV, ethmoturbinals II–IV; etr, ethmoturbinal recess; ft, frontoturbinal; it, interturbinal; lh, lamina horizontalis; lsc, lamina semicircularis; mt, marginoturbinal; mx, maxilla; mxt, maxilloturbinal; nph, nasopharyngeal duct; nt, nasoturbinal; pal, palatine.

under Bruta, alongside elephants (Proboscidea), manatees (Sirenia), sloths (Folivora), anteaters (Vermilingua), and armadillos. Later, Storr (1780) then excluded elephants and manatees to form Mutici, which became the core of Edentati, a group that included pangolins, anteaters, sloths, and armadillos (Vicq-d'Azyr 1792). Until the 20th century, pangolins were classified under Edentata, supported by Cuvier (1798). Weber (1904) classified pangolins to Pholidota within the superorder Edentata, which also included Cingulata, Folivora, Vermilingua (Xenarthra), and Tubulidentata (Afrotheria). Recent molecular studies refute these relationships, placing pangolins in Laurasiatheria and closely relating them to carnivorans (Shoshani *et al.* 1985, Murphy *et al.* 2001a, b, Meredith *et al.* 2011, O'Leary *et al.* 2013).

Studies on the nasal structures of pangolins, including turbinals and laminae, are limited and involve only a few species, mostly adults (Martinez *et al.* 2024b, Wright *et al.* 2024). Because adult turbinals and laminae are highly complex, relying solely on adults risks misidentifying homologies. Observing foetuses and neonates allows for more accurate identification by tracking the development of turbinals and laminae from simpler structures before they become complex (Maier 2014, 2000, Wagner *et al.* 2024). Developmental observations of turbinals and laminae in pangolins have not yet been conducted, and past comparisons have relied on armadillos due to previously unresolved phylogenetic relationships.

We used diffusible, iodine-based, contrast-enhanced computed tomography (diceCT) to examine foetal nasal capsules at five stages and the adult nasal cavity in *Manis pentadactyla* Linnaeus, 1758 (short-tailed pangolins). From these observations, we identified turbinals and laminae in the dry skulls of six other pangolin species. Using a phylogenetic tree built from recent molecular analyses, we then proposed evolutionary scenarios for pangolin nasal structures.

MATERIALS AND METHODS

We examined foetal specimens of *Manis pentadactyla* across five developmental stages to investigate the formation of turbinals. Additionally, we conducted prenatal observations of *Manis javanica* Desmarest, 1822 (Sunda pangolin). Molecular phylogenetic study (Gaubert *et al.* 2018) and morphological taxonomic studies (Gaudin and Wible 1999, Gaudin *et al.* 2009) have shown that pholidotans can be divided into an Asian lineage (Maninae), an African terrestrial lineage (Smutsiinae), and an African arboreal lineage (Phatagininae). Based on foetal observations, we proposed turbinal and laminae homology hypotheses for seven of eight recognized pholidotan species, though one study suggests nine (Gu *et al.* 2023): *M. pentadactyla*, *M. javanica*, *M. culionensis* de Elera, 1915 (Philippine pangolin), *Smutsia gigantea* (Illiger, 1815) (giant pangolin), *Smutsia temminckii* (Smuts, 1832) (ground pangolin), *Phataginus tricuspis* Rafinesque, 1821 (tree pangolin), and *P. tetradactyla* (Linnaeus, 1766) (long-tailed pangolin) (Fig. 2). For species besides *M. pentadactyla*, we examined adult skulls. The developmental stages and measurements for each species are presented in Tables 1 and 2. Samples were housed in the Koninklijk Museum voor Midden-Afrika (KMMA, Tervuren, Belgium), the Muséum National d'Histoire Naturelle (MNHN, Paris, France), the Natural History Museum in London (NHMUK, London, UK), the National Museum of Nature and Science (M, Tokyo, Japan), the Staatliches Museum für Naturkunde Stuttgart (SMNS, Stuttgart, Germany), the University Museum of the University of Tokyo (UMUT, Tokyo, Japan). Data for specimens housed at the American Museum of Natural History (AMNH, New York, United States) and the Smithsonian National Museum of Natural History (USNM, Washington, DC, United States) were obtained via MorphoSource (https://www.morphosource.org/).

Concerning the *M. pentadactyla* foetuses used in this study, their precise gestational age was unknown. Unlike experimental and domesticated mammals, there is no established method to estimate gestation length based on measurements such as crown–rump length (CRL) or external characteristics for pholidotans. Furthermore, the gestational length of *M. pentadactyla* varies greatly, with estimates ranging from under 166 days to over 317 days (Zhang *et al.* 2016). Consequently, determining the timing of turbinal development based on gestational duration was challenging for *M. pentadactyla*. For this study, we selected foetuses from five distinct stages with varying external morphologies to observe the development of turbinals and laminae (Fig. 3). *Manis pentadactyla* foetuses used in this study were simply numbered in order of increasing CRL and were not staged according to any established foetal staging system (Supporting Information, Fig. S1).

Furthermore, to inform hypotheses on the evolution of nasal turbinals within pholidotans among laurasiatherians, we compared previously reported species, including *Suncus murinus* (Linnaeus, 1766) (Eulipotyphla), *Rousettus leschenaultii* (Desmarest, 1820) (Chiroptera), *Sus scrofa* Linnaeus, 1758 (Cetartiodactyla), and *Felis catus* Linnaeus, 1758 (Carnivora) as documented by Ito *et al.* (2021, 2022), along with *Equus caballus* Linnaeus, 1758 (Perissodactyla), newly reported in this study. Character states of turbinals and laminae, including their number and hypotheses of loss and gain, were mapped onto the phylogenetic tree (Gaubert *et al.* 2018).

We measured CRL using sliding callipers (N20, Mitutoyo, Japan). The samples were preserved in formalin solution and subsequently transferred to 98% ethanol. We then stained the specimens using iodine-based solutions (1% iodine, I_2KI in 99% ethanol solution) following the image enhancement methods of previous studies (Gignac and Kley 2014, Gignac *et al.* 2016). The duration of staining varied from 6 to 24 h for foetuses and up to 7 days for adults, depending on specimen size.

We utilized microCT (InspeXio SMX-225CT, Shimadzu Co., Japan) to generate greyscale images of the samples. Voxel size ranged from 8 to 35 μm. Image reconstruction was performed with dimensions of 2048 × 2048 pixels and 12-bit greyscale. We manually reconstructed cartilage and bone within turbinals for each specimen using the Segmentation Editor Tool in AMIRA 5.3 (Visage Imaging, Berlin, Germany). Cartilaginous structures often showed inadequate staining with iodine-based solutions. However, they could be indirectly identified through the presence of surrounding connective tissues, such as perichondria, which readily stained with iodine-based solutions (Gignac *et al.* 2016). It was possible to differentiate ossified and cartilaginous structures from the surrounding anatomy.

Terminology

The terminology for turbinals and laminae varies among researchers, which has complicated the study of nasal cavities (Rowe *et al.* 2005, Macrini 2012, Maier and Ruf 2014, Ruf 2014). Several

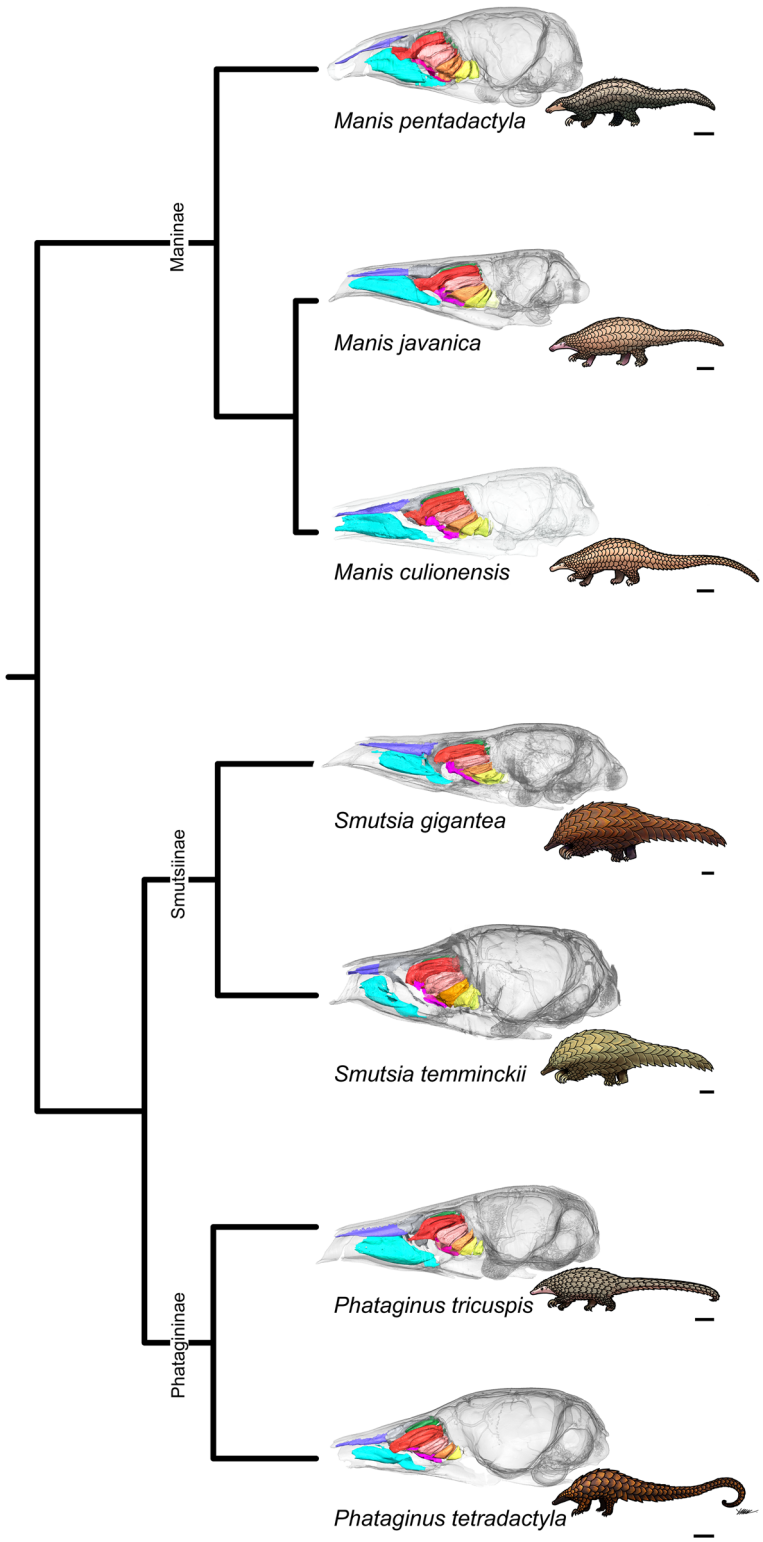

Figure 2. Phylogenetic relationships of pholidotan species included in this study. Classification of pholidotans into three groups: Asian lineage (Maninae), African terrestrial lineage (Smutsiinae), and African arboreal lineage (Phatagininae). Tree topology after Gaubert *et al.* (2018). Scale bars, 100 mm. Illustration by Miho Iwakiri.

studies have compiled the corresponding terminologies used in previous research on mammalian turbinals and laminae (Smith and Rossie 2006, 2008, Ito *et al.* 2021, 2022, Martinez *et al.* 2024a) (Supporting Information, Table S1). In this study, we adopted the anatomical terminology provided by Maier (1993a) and Voit (1909) because it encompasses the anatomical location, developmental aspects, and homology of turbinal bones (Maier and Ruf 2014).

Table 1. Distribution and the number of turbinals and laminae of pholidotans.

Species	Stage	CRL (mm)	Blanches in Maxilloturbinal	Lamina semi-circularis	Lamina horizontalis	Fronto-turbinals	Ethmo-turbinals	Structure of et I (pa) and et I (pp)	Specimen ID	Resolution (isotropic voxel size in mm)	References
Manis pentadactyla	foetal stage 1	28.6	2	X	X	5	4	shared root	M16634_a	0.008	this study
	foetal stage 2	33.41	2	X	X	5	4	shared root	M16634_b	0.011	this study
	foetal stage 3	36.67	2	X	X	5	4	shared root	M16634_c	0.012	this study
	foetal stage 4	55.53	2	X	X	5	4	shared root	M16634_d	0.018	this study
	foetal stage 5	67.39	2	X	X	5	4	shared root	M16634_f	0.019	this study
	adult	-	2	X	X	5	4	shared root	M933	0.037	this study
Manis javanica	late	70.1	2	X	X	4	5	root contact	M38361	0.021	this study
	adult	-	2	X	X	5	5	root contact	USNM: MAMM: USNM 198852	0.065	this study
Manis culionensis	adult	-	3	X	X	5	5	root separation	MNHN_1884_1822	0.025	this study
Smutsia gigantea	adult	-	3	X	X	5	5	shared root	KMMA_25479	0.072	this study
Smutsia temminckii	adult	-	3	X	X	4	4	root separation	SMNS 1077_1-2	0.018	this study
Phataginus tricuspis	adult	-	3	X	X	3	4	root separation	AMNH: Mammals: M-53874	0.047	this study
Phataginus tetradactyla	adult	-	3	X	X	4	3	root separation	NHMUK_1-11-21-35	0.046	this study

Abbreviations: et I (pa), ethmoturbinal I pars anterior; et I (pp), ethmoturbinal I pars posterior.

Table 2. Distribution and the number of turbinals and laminae of laurasiatherians.

Species		Stage	CRL	Maxillo-turbinal	Lamina semi-circularis	Lamina horizontalis	Fronto-turbinal	Ethmo-turbinals	Structure of et I (pa) and et I (pp)	Specimen ID	Resolution (isotropic voxel size in mm)	References
Suncus murinus	early	gestation day 18	8.3	X	X	X	-	3	only et I (pa)	UMUT_TSCT21041	0.006	Ito *et al.* 2022
	mid	gestation day 24	16.1	X	X	X	2	3	shared root	UMUT_TSCT21053	0.007	Ito *et al.* 2022
	late	gestation day 29	19.8	X	X	X	2	3	shared root	UMUT_Suncus_KI02	0.007	Ito *et al.* 2021
	adult	-	-	X	X	X	2	3	shared root	UMUT_KATS_835A	0.022	Ito *et al.* 2022
Rousettus leschenaultii	early	gestation day 60 (CS 18)	7.4	X	X	X	-	1	only et I (pa)	VN17-366	0.009	Ito *et al.* 2021
	mid	gestation day 65 (CS 19)	9.6	X	X	X	1	3	shared root	VN17-357	0.012	Ito *et al.* 2021
	late	gestation day 85 (CS 23)	13.5	X	X	X	1	3	shared root	VN18-45	0.016	Ito *et al.* 2021
	adult	-	-	X	X	X	1	3	shared root	UMUT_KI19-001_sl41	0.031	Ito *et al.* 2021
Sus scrofa	mid	gestation day 28	17.9	X	X	X	1	2	only et I (pa)	UMUT_Pig_K013_KI_CRL18	0.011	Ito *et al.* 2021
	late	gestation day 40	42.4	X	X	X	3	4	shared root	UMUT_Pig_K76_KI_CRL42	0.016	Ito *et al.* 2021
	adult	-	-	X	X	X	4	6	shared root	-	-	Paulli 1900b
Equus caballus	mid	-	154	X	X	X	3	5	shared root	-	0.020	this study
Felis catus	mid	gestation day 38	58.8	X	X	X	3	3	shared root	UMUT_Cat_K025_KI_CRL59	0.018	Ito *et al.* 2021
	late	gestation day 49	99.5	X	X	X	3	3	shared root	UMUT_Cat_K025_KI_CRL100	0.035	Ito *et al.* 2021
	adult	-	-	X	X	X	3	3	shared root	-	-	Paulli 1900c

Abbreviations: et I (pa), ethmoturbinal I pars anterior; et I (pp), ethmoturbinal I pars posterior.

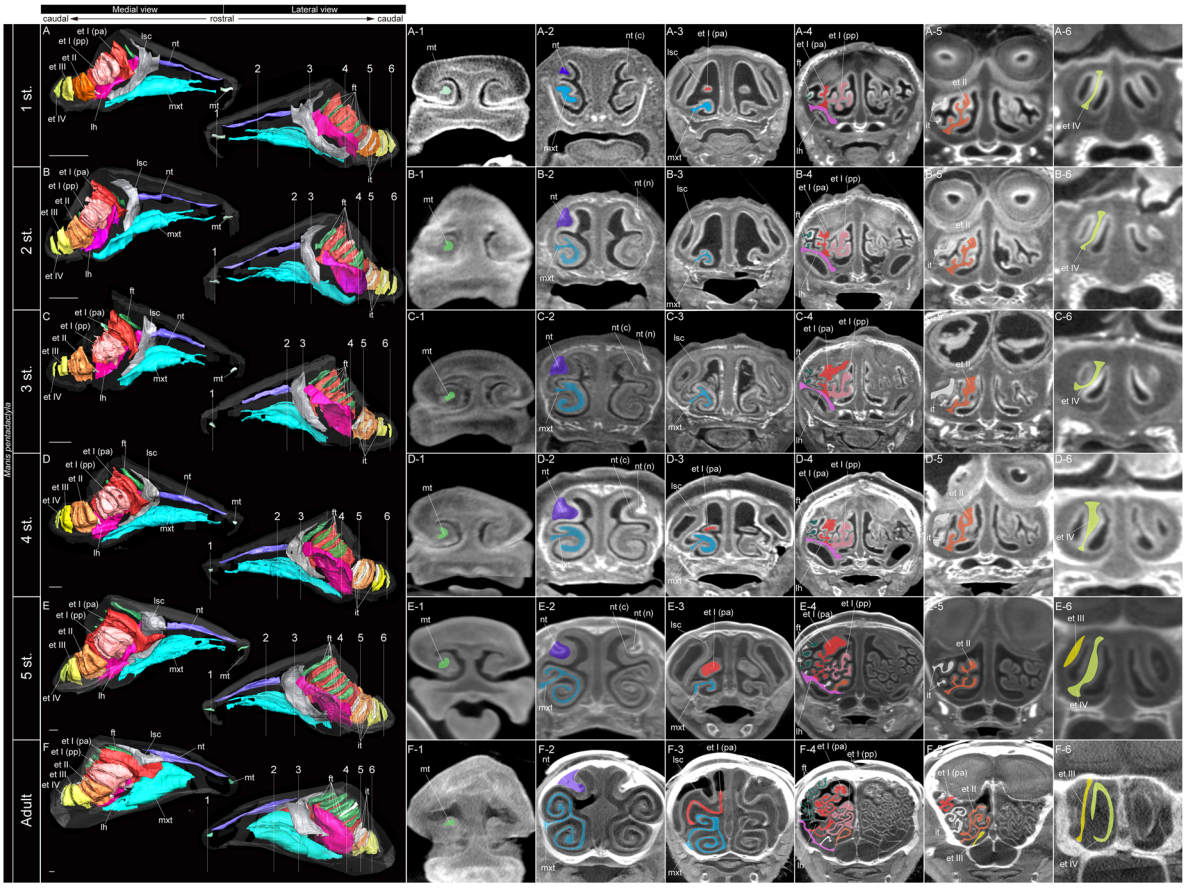

Figure 3. Coronal section of diceCT images of *Manis pentadactyla*. (1–6) show approximate location of section through the nasal capsule or nasal cavity. (A1–6) foetal stage 1, (B1–6) foetal stage 2, (C1–6) foetal stage 3, (D1–6) foetal stage 4, (E1–6) foetal stage 5, and (F1–6) adult of *M. pentadactyla*. Scale bars, 1mm. Abbreviations: et I (pa), ethmoturbinal I pars anterior; et I (pp), ethmoturbinal I pars posterior; et II–III, ethmoturbinal II–III; ept, epiturbinal; ft, frontoturbinal; it, interturbinal; lh, lamina horizontalis; lsc, lamina semicircularis; mt, marginoturbinal; mxt, maxilloturbinal; nt, nasoturbinal; nt(c), nasoturbinal from cartilage; nt(n), nasoturbinal from nasal bone.

RESULTS

Marginoturbinal and atrioturbinal

Within the pholidotans, we observed the cartilaginous external nose of *M. pentadactyla* foetuses and adults after iodine staining and CT scanning. The marginoturbinal and atrioturbinal in the external nose consisted of thin cartilage with no ossification observed (Fig. 3A-1, B-1, C-1, D-1, E-1, F-1). In both the foetuses and adults of *M. pentadactyla*, the marginoturbinal was positioned most rostrally and scrolled weakly ventrally. The marginoturbinal of *M. pentadactyla* began to scroll inward from foetal stage 1 (Fig. 3A-1). As it progressed from the foetal stage 5 to adult, the marginoturbinal appeared relatively small compared to the size of the external nose (Fig. 3E-1). The dorsal scrolling of the marginoturbinal also became more pronounced. The structures between the marginoturbinal and atrioturbinal, and between the atrioturbinal and maxilloturbinal, were indistinct. From the foetal stage 1 of *M. pentadactyla*, an extended ventral maxilloturbinal began along the caudal extension line of the marginoturbinal. In adult *M. pentadactyla*, there was a wider space between the marginoturbinal and maxilloturbinal (Fig. 3F-1).

The marginoturbinal of the late-stage foetus of *M. javanica* exhibited similar structures to those of the foetal stage 5 of *M. pentadactyla* (Figs 3E-1, 4A-1). These were thin cartilaginous structures, with no evidence of ossification. The ventral maxilloturbinal, extending rostrally, began along the caudal extension of the marginoturbinal (Fig. 4A-1).

For other pholidotan species, only prepared dry skulls were CT-scanned; therefore, the cartilaginous marginoturbinal and atrioturbinal were not preserved (Fig. 5).

In the foetuses and adults of *S. murinus*, *R. leschenaultii*, as well as the foetuses of *S. scrofa*, *F. catus*, and *E. caballus*, the marginoturbinal was located ventrally (Fig. 6). As their development progressed, the dorsal scrolling of their marginoturbinal became more pronounced. Clear contrasts with surrounding soft tissues were not established, resulting in them being not distinctly visible. In particular, the structures between the marginoturbinal and atrioturbinal, and between the atrioturbinal and maxilloturbinal, were not discernible in any species. In the foetuses and adults of all species, the marginoturbinal and atrioturbinal were positioned rostrally to the maxilloturbinal (Fig. 6).

Maxilloturbinal

In both the foetuses and adults of *M. pentadactyla*, the marginoturbinal was located anteriorly to the ventrally extended anterior portion of the maxilloturbinal (Fig. 3). While the maxilloturbinal lies on the extension line of the marginoturbinal, a gap existed

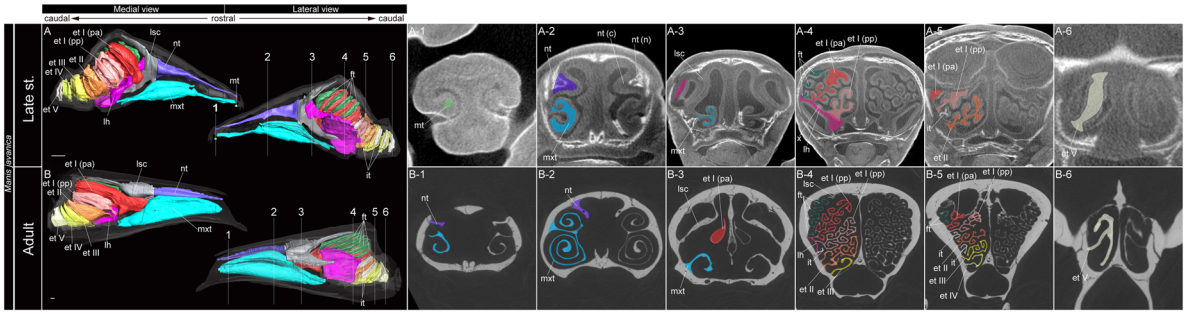

Figure 4. Coronal section of diceCT and μCT images of *Manis javanica*. (1–6) show approximate location of section through the nasal capsule or nasal cavity. (A1–6) Late stage foetus and (B1–6) adult of *M. javanica*. Scale bars, 1mm. Abbreviations: et I (pa), ethmoturbinal I pars anterior; et I (pp), ethmoturbinal I pars posterior; et II–III, ethmoturbinal II–III; ept, epiturbinal; ft, frontoturbinal; it, interturbinal; lh, lamina horizontalis; lsc, lamina semicircularis; mt, marginoturbinal; mxt, maxilloturbinal; nt, nasoturbinal.

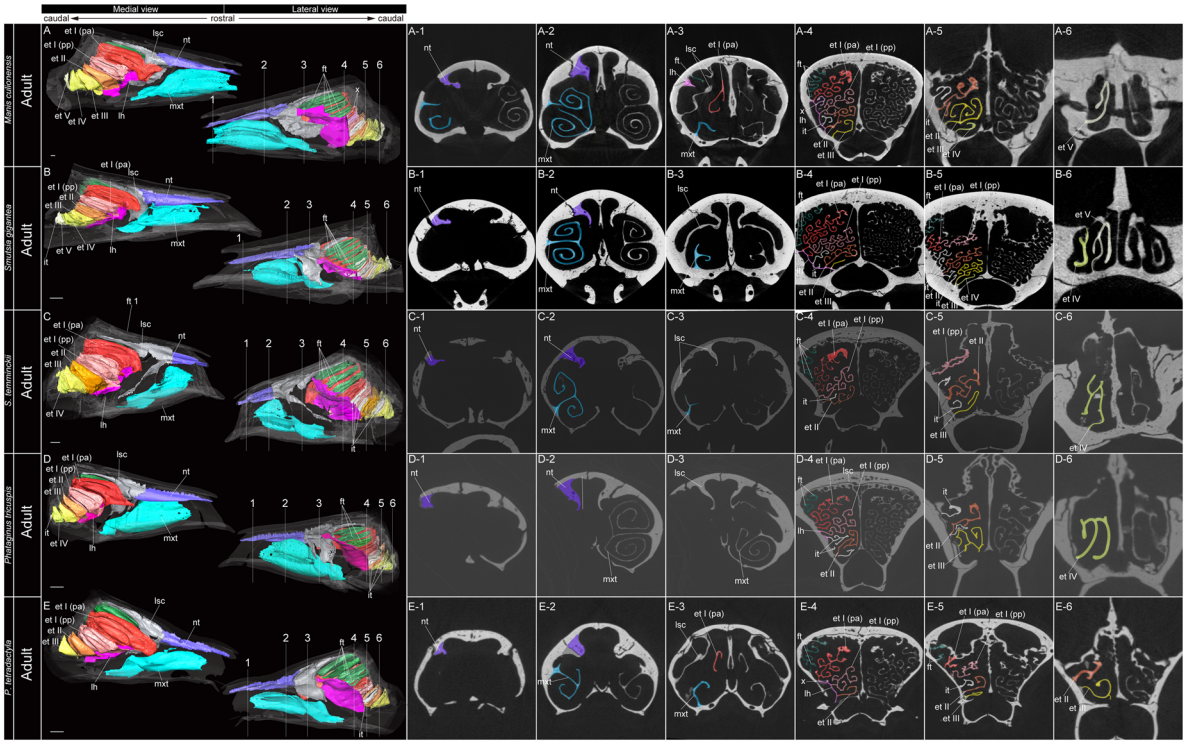

Figure 5. Coronal section of μCT images of adult pholidotan species. (1–6) show approximate location of section through the nasal cavity: (A1–6) *M. culionensis*, (B1–6) *Smutsia gigantea*, (C1–6) *S. temminckii*, (D1–6) *Phataginus tricuspis*, and (E1–6) *P. tetradactyla*. Scale bars, 1mm. Abbreviations: et I (pa), ethmoturbinal I pars anterior; et I (pp), ethmoturbinal I pars posterior; et II–III, ethmoturbinal II–III; ept, epiturbinal; ft, frontoturbinal; it, interturbinal; lh, lamina horizontalis; lsc, lamina semicircularis; mt, marginoturbinal; mxt, maxilloturbinal; nt, nasoturbinal; x, uncertain.

between these turbinals (Fig. 3). From foetal stage 1 to stage 5, the ventral part of the maxilloturbinal consistently projected anteriorly (Fig. 3A–E). However, from foetal stage 3 onward to adult, the dorsal part of the maxilloturbinal also began to project anteriorly (Fig. 3C–F). In foetal stage 1, the middle section of the maxilloturbinal had already bifurcated into two parts (Fig. 3A-2). These two branches, one dorsal and the other ventral, curled outward (Fig. 3A-2, B-2, C-2, D-2, E-2, F-2). The degree of this curling intensified from foetal stage 1 to adult (Fig. 3A–F). From foetal stage 2 onward, the two branched sections, dorsal and ventral, of the maxilloturbinal displayed the ventral section curling in a more pronounced arc (Fig. 3B-2, C-2, D-2, E-2, F-2). In the adult, the ventral portion of the maxilloturbinal was more prominently developed (Fig. 3F-2). The caudal part of maxilloturbinal in foetal stage 1 only had the ventral branch formed, with the dorsal branch absent (Fig. 3A, A-2). This ventral branch in foetal stage 1 had a bent structure but started curling ventrally from foetal stage 2 onward (Fig. 3B-2, C-2, D-2, E-2, F-2). This curling became more pronounced with development. The utmost caudal part of the maxilloturbinal, from foetal stage 1 to adult, maintained an inward projection and, despite developmental progression, did not exhibit curling.

The maxilloturbinal of the late-stage foetus of *M. javanica* displayed a similar structure to that of the foetal stage 5 of *M.*

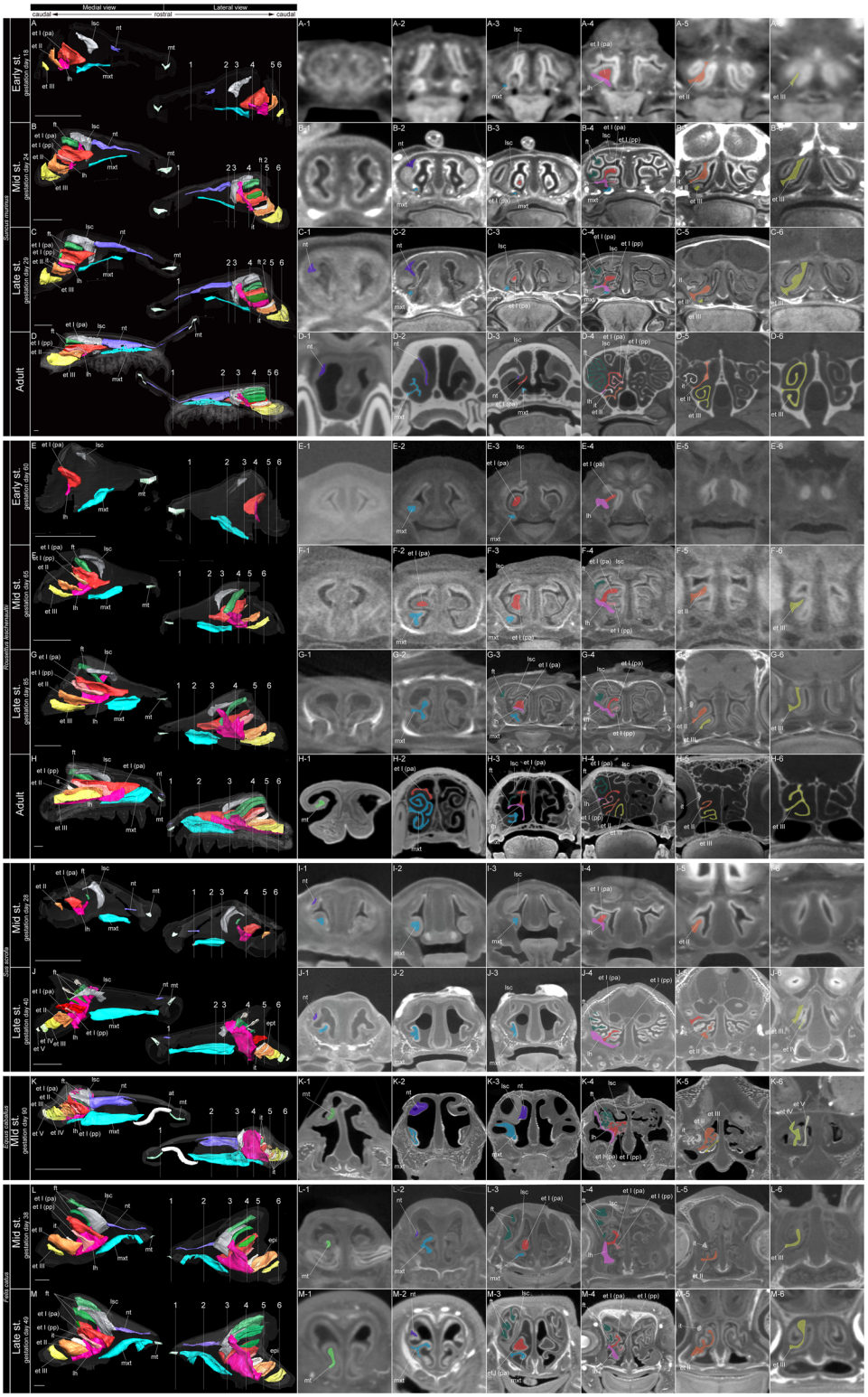

Figure 6. Coronal section of μCT images of *Suncus murinus* (Eulipotyphla), *Rousettus leschenaultii* (Chiroptera), *Sus scrofa* (Cetartiodactyla), *Equus caballus* (Perissodactyla), and *Felis catus* (Carnivora). (1–6) show approximate location of section through the nasal capsule or nasal cavity. (A1–6) early-stage foetus, (B1–6) mid-stage foetus, (C1–6) late-stage foetus, (D1–6) adult of *S. murinus*, (E1–6) early-stage foetus, (F1–6) mid-stage foetus, (G1–6) late-stage foetus, (H1–6) adult of *R. leschenaultii*; (I1–6) mid-stage foetus, and (J1–6) late-stage foetus of *S. scrofa*, (K1–6) late-stage foetus of *E. caballus*; (L1–6) mid-stage foetus, and (M1–6) late-stage foetus of *F. catus*. Scale bars, 1mm. Abbreviations: et I (pa), ethmoturbinal I pars anterior; et I (pp), ethmoturbinal I pars posterior; et II–III, ethmoturbinal II–III; ept, epiturbinal; ft, frontoturbinal; it, interturbinal; lh, lamina horizontalis; lsc, lamina semicircularis; mt, marginoturbinal; mxt, maxilloturbinal; nt, nasoturbinal.

pentadactyla (Figs 3E, 4A). In the rostral region, the ventral branch of the maxilloturbinal, which may include the atrioturbinal, projected rostrally (Fig. 4A). In the middle region of the maxilloturbinal, the two branches—dorsal and ventral—scrolled outward. The ventral branch scrolled into a more pronounced arc (Fig. 4A-2, B-2).

Furthermore, adult individuals of other pholidotans exhibited maxilloturbinals with structures similar to those of adult *M. pentadactyla* and *M. javanica* (Figs 3, 4). Specifically, from the middle to the caudal part of the maxilloturbinal, the ventral branches were prominent, and at the caudal end, the dorsal branches disappeared, leaving only the ventral branches, which showed strong coiling (Fig. 5). In *S. gigantea*, *S. temminckii*, *P. tricuspis*, and *P. tetradactyla*, short branches protruded dorsally from the dorsal side of the root of the maxilloturbinal (Fig. 5B-3, C-3, D-3, E-2). In *S. gigantea*, these short branches were fused with the rostral part of the lamina semicircularis (Fig. 5B). In *M. culionensis* as well, short branches protruded dorsally from the dorsal side of the root, but they were quite small (Fig. 5A-3).

In all outgroups, the maxilloturbinal developed on the ventral side of the nasal capsule (Fig. 6). From the mid- to late-stages of *S. murinus*, there was a ventrally scrolled maxilloturbinal. Its tip did not bifurcate but merely swelled (Fig. 6A-3–C-3). In adult *S. murinus*, it bifurcated into two branches, with both the dorsal and ventral sides strongly scrolled. An additional short branch protruded from the dorsal side (Fig. 6D-2). In the early-stage of *R. leschenaultii*, a depression was observed at the tip of the middle part of the maxilloturbinal (Fig. 6E-2). From the mid-stage of *R. leschenaultii*, the maxilloturbinal formed secondary lamellae on both the dorsal and ventral sides (Fig. 6F-2). In adult *R. leschenaultii*, tertiary projections emerged from both the ventral and dorsal lamellae. The nasal capsule formed a total of four lamellae (Fig. 6H-2). In the mid-stage of *S. scrofa*, the maxilloturbinal formed secondary lamellae on both the dorsal and ventral sides (Fig. 6I-2). In the late-stage of *S. scrofa*, both secondary lamellae were scrolled outward (Fig. 6J-2). In the mid-stage of *E. caballus*, the maxilloturbinal scrolled dorsally but did not form secondary lamellae (Fig. 6K-2, K-3). In *F. catus*, from the mid-stage, the maxilloturbinal formed secondary lamellae on both dorsal and ventral sides (Fig. 6L-2). In the late-stage of *F. catus*, the scrolling of the ventral lamellae became more pronounced than the dorsal lamellae (Fig. 6M-2).

Nasoturbinal

From foetal stage 1 to adult in *M. pentadactyla*, the nasoturbinal was a protruding structure extending from the dorsal to the ventral direction of the cavity, presenting a long structure from the rostral to caudal end (Fig. 3). In foetal stage 1, the nasoturbinal was a cartilaginous structure protruding from the inner wall of the nasal capsule (Fig. 3A-2; Supporting Information, Fig. S2A-2). However, from foetal stage 2, the dorsal side of the nasal capsule started to curve, protruding into the nasal cavity in a pronounced arc. Concurrently, projections formed by the nasal bone began to extend in a ventral direction (Fig. 3B-2; Supporting Information, Fig. S2B-2). From foetal stage 4, the projections formed by the nasal bone penetrated the large curve protruding into the cavity from the dorsal side of the nasal capsule (Fig. 3D-2; Supporting Information, Fig. S2D-2). In adults, the nasoturbinal derived from the nasal capsule and the nasoturbinal originating from the nasal bone had completely fused and ossified (Fig. 3F-2; Supporting Information, Fig. S2, S2F-2). The rostral part of the nasoturbinal remained cartilaginous from the foetal stage 1 to adult (Supporting Information, Fig. S2A-1, B-1, C-1, D-1, E-1, F-1). From foetal stage 1, the caudal part of the nasoturbinal was fused with the rostral part of the lamina semicircularis (Fig. 3).

The structure of the nasoturbinal from the late-stage foetus to the adult *M. javanica* was similar to that of *M. pentadactyla* (Figs 3E, F, 4A, B). In the late-stage foetus, the nasoturbinal derived from the nasal capsule formed a large curve toward the nasal cavity, with the nasoturbinal derived from the nasal bone embedded within this curve (Fig. 4A-2). In adults, the nasoturbinal from the nasal capsule ossified and fused with the nasal bone-derived structure (Fig. 4B-2). Alternatively, it is possible that the nasoturbinal from the nasal capsule remained cartilaginous and merged with the external nose. In this case, it would have disappeared during the preparation of skeletal specimens.

In this study, in other adult pholidotans, the rostral part of the nasoturbinal—thought to be located in the external nose—was not observed (Fig. 5A–E). However, the ossified nasoturbinal of these species exhibited a structure similar to that of adult *M. pentadactyla* and *M. javanica*. Specifically, the nasoturbinal protrudes from the dorsal to the ventral direction within the nasal cavity, extending longitudinally from the rostral to the caudal side (Figs 3–5).

Within the outgroup, *S. murinus* exhibited a dorsal protrusion forming from the nasal capsule near the nostrils at the early-stage (Fig. 6A). From the mid- to late-stages, the nasoturbinal, which did not include rostral cartilage, extended caudally, and from the tectum located dorsally on the caudal nasal capsule, the nasoturbinal projected inward into the cavity (Fig. 6B-1, C). In the adult, most of the rostral portion of the nasoturbinal near the external nose was ossified, except for a segment that remained unossified (Fig. 6D-1, D-2). In *R. leschenaultii*, the nasoturbinal was not observed from the early- to late-stages (Fig. 6E-1, F-1, G-1). However, a non-cartilaginous protrusion, thought to represent the nasoturbinal, was present on the dorsal inner wall near the nostrils (Fig.6H-1). In *S. scrofa*, a protrusion forming the nasoturbinal appeared from the dorsal part of the nasal capsule near the nostrils (on the inner wall of the rostral tectum nasi anterius) starting from the mid-stage (Fig. 6I-1, J-1). In *E. caballus*, at the mid-stage, the nasoturbinal derived from the nasal capsule showed a significant curve toward the nasal cavity, with the nasoturbinal originating from the nasal bone wedged into this curve (Fig. 6K-2). In *F. catus*, from the mid-stage onward, a protrusion from the nasal cavity side of the rostral tectum nasi anterius extended caudally and fused with the lamina semicircularis (Fig. 6L, L-2, M, M-2).

Lamina semicircularis

In *M. pentadactyla* at foetal stage 1, the lamina semicircularis bridged dorsoventrally in the middle portion of the nasal capsule and formed a structure that expanded dorsoventrally in the caudal region (Fig. 3A-3). The rostralmost part of the lamina semicircularis fused with the nasoturbinal (Fig. 3A–F). Starting from foetal stage 2, the middle portion of the lamina semicircularis bent

inward toward the cavity (Fig. 3B-3, C-3, D-3, E-3). From foetal stage 5, the caudal part of the lamina semicircularis expanded dorsoventrally (Fig. 3E-3). In adults, the ventral part of the lamina semicircularis formed an S-shaped structure in coronal view, with the ventral portion pushed dorsally. Additionally, a short branch projecting laterally was observed on the dorsal side of the lamina semicircularis (Fig. 3F-3).

The structure of the lamina semicircularis from the late-stage foetus to the adult *M. javanica* was similar to that from foetal stage 5 to the adult *M. pentadactyla* (Figs 3E-3, F-3, 4A-3, B-3).

The lamina semicircularis of adult pholidotans also showed a basic structure consistent with that of adult *M. pentadactyla* and *M. javanica*, with an S-shaped structure in coronal view formed by the ventral part being pushed dorsally, and a short lateral branch observed on the dorsal side (Figs 3F-3, 4B-3, 5A-3, B-3, D-3, E-3).

In *S. murinus*, at the early-stage, the lamina semicircularis formed a structure that expanded dorsoventrally from the dorsal side of the caudal nasal capsule (Fig. 6A-3). From the mid- to late-stages, it expanded dorsoventrally, covering the lamina horizontalis and the frontoturbinals (Fig. 6B, C). In adult *S. murinus*, it ossified in the rostral nasal cavity, bridging from the dorsal to the ventral side (Fig. 6D-3).

In *R. leschenaultii*, at the early-stage, the lamina semicircularis protruded dorsally from the nasal capsule (Fig. 6E-3). From the mid- to late-stages, it rose outward, and in the adult, the lateral tip slightly scrolled dorsally (Fig. 6F-3, G-3, H-3).

In *S. scrofa*, during the mid-stage, the lamina semicircularis projected into the cavity from the dorsal side of the nasal capsule (Fig. 6I-3). During the late-stage, the rostral part of the lamina semicircularis bridged outward from the dorsal nasal capsule, while the caudal part of the lamina semicircularis expanded dorsally toward the cavity (Fig. 6J-3).

In *E. caballus*, at the mid-stage, the lamina semicircularis projected into the cavity from the dorsal nasal capsule, with the rostral part bridging the dorsal section of the nasal capsule, but it was smaller compared to the other outgroups. The caudal part of the lamina semicircularis scrolled outward (Fig. 6K-3, K-4).

In *F. catus*, from the mid-stage, the rostral lamina semicircularis bridged outward from the dorsal nasal capsule (Fig. 6L-3, M-3).

Lamina horizontalis

In foetal stage 1 of *M. pentadactyla*, the dorsal side of the lamina horizontalis was fused with ethmoturbinal I pars anterior, pars posterior, and the interturbinal (the dorsal interturbinal located between pars posterior and ethmoturbinal II), as well as the ventralmost and second ventralmost frontoturbinals, projecting into the nasal cavity (Fig. 3A). Additionally, the caudal region of the lamina horizontalis fused ventrally with the caudal part of the maxilloturbinal, forming the maxilloturbinal recess (Fig. 3A-4).

Starting from foetal stage 2, the dorsal region of the lamina horizontalis was fused with ethmoturbinal II (Fig. 3B). In the adult, the lamina horizontalis expanded dorsoventrally and was already fused with ethmoturbinal I pars anterior, pars posterior, and interturbinals (both dorsal and ventral interturbinals between ethmoturbinal I pars posterior and ethmoturbinal II), as well as the ventralmost, second ventralmost, and third ventralmost frontoturbinals (Fig. 3F).

In late-stage foetuses and adults of *M. javanica*, the dorsal side of the lamina horizontalis was fused with ethmoturbinal I pars anterior, ethmoturbinal I pars posterior, and the epiturbinal located closest to the roof of the ethmoturbinal I pars anterior among the multiple epiturbinals associated with it. The lamina horizontalis was also fused with the interturbinal located between ethmoturbinal I pars posterior and ethmoturbinal II, ethmoturbinal II, as well as the ventralmost and second ventralmost frontoturbinals (Fig. 4A, B).

In adults of all pholidotan species, the lamina horizontalis expanded dorsoventrally, dividing the nasal cavity into dorsal and ventral spaces from the mid to the caudal part of the nasal cavity (Fig. 5). In *M. culionensis*, the dorsal side of the lamina horizontalis was fused with several structures, including ethmoturbinal I pars anterior, a presumed ethmoturbinal I pars posterior, and a structure located between ethmoturbinal I pars anterior and pars posterior, thought to represent the epiturbinal of ethmoturbinal I pars anterior. Additionally, it was fused with the interturbinal located between ethmoturbinal I pars posterior and ethmoturbinal II, ethmoturbinal II, as well as the ventralmost and second ventralmost frontoturbinals (Fig. 5A).

In *S. gigantea*, the dorsal side of the lamina horizontalis was fused with the shared root of ethmoturbinal I pars anterior and pars posterior. It was also fused with a structure thought to represent the epiturbinal of ethmoturbinal I pars anterior. Additionally, it was fused with two interturbinals positioned between ethmoturbinal I pars posterior and ethmoturbinal II, with the ventral interturbinal possibly representing the epiturbinal of ethmoturbinal II. Fusion was also observed with ethmoturbinal II, ethmoturbinal III, and the ventralmost frontoturbinal (Fig. 5B).

In *S. temminckii*, the dorsal side of the lamina horizontalis fused with several structures. These included ethmoturbinal I pars anterior, a structure believed to be ethmoturbinal I pars posterior, and an uncertain structure located between ethmoturbinal I pars anterior and ethmoturbinal I pars posterior. The latter is possibly an interturbinal or an epiturbinal of ethmoturbinal I pars anterior (Fig. 5, C-4). Fusion was also observed with an interturbinal located between ethmoturbinal I pars posterior and ethmoturbinal II, ethmoturbinal II, and the ventralmost frontoturbinal (Fig. 5C).

In *P. tricuspis*, the dorsal side of the lamina horizontalis was fused with several structures. These included ethmoturbinal I pars anterior, a structure presumed to be ethmoturbinal I pars posterior, and an uncertain structure located between ethmoturbinal I pars anterior and ethmoturbinal I pars posterior, which may correspond to an interturbinal or an epiturbinal. Additionally, fusion was observed with two interturbinals located between ethmoturbinal I pars posterior and ethmoturbinal II, as well as with ethmoturbinal II and the ventralmost frontoturbinal (Fig. 5D).

In *P. tetradactyla*, the dorsal side of the lamina horizontalis was fused with ethmoturbinal I pars anterior, a structure believed to be ethmoturbinal I pars posterior, the interturbinal between ethmoturbinal I pars posterior and ethmoturbinal II, ethmoturbinal II, and the ventralmost frontoturbinal (Fig. 5E).

In *S. murinus*, at the early-stage, the dorsal side of the lamina horizontalis was already fused with the ventral sides of ethmoturbinal I and ethmoturbinal II, projecting into the nasal cavity (Fig. 6A). From the mid-stage to adult, the dorsal side of the lamina horizontalis extended both dorsally and ventrally, connecting with the ventral side of ethmoturbinal I pars anterior. It also connected with the ventral sides of two frontoturbinals and extended inward, encompassing these structures (Fig. 6B–D).

In *R. leschenaultii*, at the early-stage, the lamina horizontalis projected from the inner wall of the nasal capsule, connecting with the ventral side of ethmoturbinal I pars anterior (Fig. 6E). From the mid-stage to adult, the dorsal side of the lamina horizontalis connected with the ventral sides of ethmoturbinal I pars anterior, ethmoturbinal II, ethmoturbinal III, and two frontoturbinals, projecting from the inner wall of the nasal capsule (Fig. 6F–H).

In *S. scrofa*, from the mid- to late-stages, the lamina horizontalis projected horizontally from the inner wall of the nasal capsule, connecting with the ventral side of ethmoturbinal I pars anterior. Additionally, at the mid-stage, the dorsal side of the lamina horizontalis connected with the ventral sides of ethmoturbinal I pars posterior, ethmoturbinal II, three frontoturbinals, and an interturbinal (Fig. 6I, J).

In *E. caballus*, at the mid-stage, the lamina horizontalis projected vertically from the inner wall of the nasal capsule, connecting with the ventral side of ethmoturbinal I pars anterior. The dorsal side of the lamina horizontalis also connected with ethmoturbinal II, three frontoturbinals, and an interturbinal located between ethmoturbinal I and ethmoturbinal II (Fig. 6K).

In *F. catus*, from the mid- to late-stages, the dorsal side of the lamina horizontalis connected with the ventral sides of ethmoturbinal I pars anterior, ethmoturbinal I pars posterior, ethmoturbinal II, three frontoturbinals, and an interturbinal, projecting from the inner wall (Fig. 6L, M).

Frontoturbinal recesses

In *M. pentadactyla*, at foetal stage 1, four frontoturbinals projected from the inner wall of the nasal capsule (Fig. 3A-4; Table 1). From foetal stage 2 to stage 5, the inner sides of all frontoturbinals expanded (Fig. 3B-4, C-4, D-4, E-4). In adults, the inner sides of all frontoturbinals bifurcated and scrolled outward (Fig. 3F-4). A septum dividing the frontoturbinal recesses was not observed from the foetal to adult (Fig. 3A-4, B-4, C-4, D-4, E-4, F-4).

The late-stage foetus of *M. javanica* displayed a structure similar to that of foetal stage 5 in *M. pentadactyla* (Figs 3E, F, 4A, B). In adult *M. javanica*, the number of frontoturbinals increased to five, each bifurcating on the inner side and scrolling inward toward the inner wall (Fig. 4B-1; Table 1). No septum that would partition the frontoturbinal recesses was observed (Fig. 4A-1, B-1).

In adults of other species, the inner bifurcation and outward scrolling morphology of the frontoturbinals were consistent, though the number of frontoturbinals varied (Fig. 5; Table 1). Observed counts included five frontoturbinals in *M. culionensis* (Fig. 5A; Table 1), five in *S. gigantea*, along with three additional small structures of uncertain classification (either small frontoturbinals or interturbinals) (Fig. 5B; Table 1), four in *S. temminckii* (Fig. 5C; Table 1), three in *P. tricuspis* (Fig. 5D; Table 1), and four in *P. tetradactyla* (Fig. 5E; Table 1). No septum dividing the frontoturbinal recesses was observed in any species (Fig. 5A-4, B-4, C-4, D-4, E-4).

In *S. murinus*, no frontoturbinal protrusions were observed at the early-stage. From the mid- to late-stages, two frontoturbinals (dorsal and ventral) projected from the dorsal side of the inner wall of the nasal capsule (Fig. 6B-4, C-4). In the adult, both frontoturbinals scrolled outward (Fig. 6D-4).

In *R. leschenaultii*, a frontoturbinal projected from the dorsal side of the inner wall of the nasal capsule from the mid-stage to adult (Fig. 6F-4, G-4, H-4). In the adult, the single frontoturbinal scrolled dorsally (Fig. 6H-4).

In *S. scrofa*, at the mid-stage, a dorsal frontoturbinal slightly projected from the dorsal side of the inner wall of the nasal capsule (Fig. 6I). Additionally, three frontoturbinals projected from the inner wall of the nasal capsule at the late stage (Fig. 6J).

In *E. caballus*, at the mid-stage, three frontoturbinals slightly projected from the dorsal side of the inner wall of the nasal capsule. Structures resembling interturbinals were observed between the most dorsal frontoturbinal and the lamina semicircularis, between the most ventral frontoturbinal and ethmoturbinal I pars anterior, and between each frontoturbinal (Fig. 6K).

In *F. catus*, at the mid-stage, three frontoturbinals were already projecting from the dorsal side of the inner wall of the nasal capsule (Fig. 6L; Table 2). By the late-stage, the innermost tips of each frontoturbinal had begun to bifurcate (Fig. 6M).

Ethmoturbinal I pars anterior

In foetal stage 1 of *M. pentadactyla*, the ethmoturbinal I pars anterior protruded into the nasal cavity from the inner wall of the nasal capsule and was dorsally connected with the lamina horizontalis. The ethmoturbinal I pars anterior extended in both the lateromedial and caudorostral directions, with the ethmoturbinal I pars posterior splitting from its ventral side (Fig. 3A-4). The rostral tip of the ethmoturbinal I pars anterior was flattened (Fig. 3A-3). From the foetal stages 1 to 4, the ethmoturbinal I pars anterior had eight epiturbinals, increasing to nine in foetal stage 5. Additionally, from foetal stage 5 onward, the rostral portion of the ethmoturbinal I pars anterior showed a protrusion directed toward the nostril (Fig. 3E, F). In adults, the rostral portion formed a flat structure oriented mediolaterally, passing between the maxilloturbinal and the lamina semicircularis. The outer side of the rostral portion scrolled inward, while the inner side scrolled outward (Fig. 3F-3). Throughout all foetal stages and in adults, the ethmoturbinal I pars anterior remained the largest turbinal (Fig. 3).

In the late-stage foetus of *M. javanica*, the ethmoturbinal I pars anterior had eight epiturbinals. However, in the adult, only seven epiturbinals were present dorsally (Fig. 4A-1). In the late-stage foetus of *M. javanica*, four frontoturbinals are present, whereas five are found in the adult. This difference suggests that the epiturbinal situated at the most basal dorsal position of the ethmoturbinal I pars anterior in the late-stage foetus may later differentiate into an additional frontoturbinal; alternatively, one of the dorsal epiturbinals of the ethmoturbinal I pars anterior may regress.

In adults of other species, the rostral portion of the ethmoturbinal I pars anterior showed little difference from that of adult *M. pentadactyla* and *M. javanica* (Figs 3–5). The rostral part of the

ethmoturbinal I pars anterior formed a flat structure oriented mediolaterally, passing between the maxilloturbinal and the lamina semicircularis (Fig. 5A–E). The outer side scrolled inward, while the inner side scrolled outward. The main variation observed was in the number of epiturbinals, with *S. gigantea* having the most at 11 and *P. tricuspis* and *P. tetradactyla* having the fewest at seven.

In *S. murinus*, the ethmoturbinal I pars anterior fuses dorsally with the lamina horizontalis while protruding from the inner wall of the nasal capsule in lateral–medial and caudal–rostral directions from the early-stage (Fig. 6A–D, A-4, B-4, C-4, D-4). From mid-stage to adult, its rostral portion extends toward the naris (Fig. 6B–D). In *R. leschenaultii* (early-stage), *S. scrofa* (mid-stage), and *E. caballus*, the ethmoturbinal I pars anterior similarly protrudes from the inner wall and fuses with the dorsal side of the lamina horizontalis (Fig. 6E, E-4, I, I-4, K, K-4). In *F. catus*, it shows the same pattern at the mid-stage, and at the late-stage, its medial end begins to divide (Fig. 6L, L-4, M, M-4). In all outgroup species examined, the ethmoturbinal I pars anterior is the largest ethmoturbinal at every developmental stage.

Ethmoturbinal I pars posterior

In *M. pentadactyla*, the ethmoturbinal I pars posterior divided from the ventral side of the ethmoturbinal I pars anterior, and from foetal stage 1, its innermost part showed a prominent bifurcation (Fig. 3A-4, B-4, C-4, D-4, E-4). In adults, all laminae, except the most dorsal one, bifurcated and scrolled individually.

In the late-stage foetus of *M. javanica*, a structure believed to be the ethmoturbinal I pars posterior appeared ventrally, seemingly independent of the ethmoturbinal I pars anterior (Fig. 4A-4). Between the ethmoturbinal I pars anterior and the structure presumed to be the ethmoturbinal I pars posterior, a projection was observed, possibly an epiturbinal of the ethmoturbinal I or an interturbinal (Fig. 4A-4). In the adult, the ethmoturbinal I pars posterior protruded from the root of the ethmoturbinal I pars anterior (Fig. 4B, B-4).

In adults of other species, the location of the ethmoturbinal I pars posterior varied (Fig. 5). Among them, only *S. gigantea* showed the same splitting position as in *M. pentadactyla*, with the ethmoturbinal I pars anterior and the ethmoturbinal I pars posterior sharing a common root (Figs 3F-4, 5B-4; Table 1). In *S. temminckii*, *P. tricuspis*, and *P. tetradactyla*, the ethmoturbinal I pars posterior protruded from the root of the ethmoturbinal I pars anterior on the inner nasal wall (Fig. 5C-4, D-4, E-4; Table 1). In *M. culionensis*, the ethmoturbinal I pars posterior projects from a more ventral position, further from the root of the ethmoturbinal I pars anterior than in *S. temminckii*, *P. tricuspis*, or *P. tetradactyla* (Fig. 5A-4, C-4, D-4, E-4; Table 1). Between the ethmoturbinal I pars anterior and the structure presumed to be the ethmoturbinal I pars posterior, a small turbinal of uncertain identification (either an interturbinal or an epiturbinal of the ethmoturbinal I) was observed (Fig. 5A-4, E-4). The identification of the ethmoturbinal I pars posterior in *M. culionensis* is hypothetical, as it cannot be completely ruled out that this structure might be the ethmoturbinal II.

In *S. murinus*, the ethmoturbinal I pars posterior was not observed at the early-stage (Fig. 6A). From the mid-stage onward, the ethmoturbinal I pars posterior and the ethmoturbinal I pars anterior shared a common root (Fig. 6B, C). In the adult, the tip of the ethmoturbinal I pars posterior bifurcated. In *R. leschenaultii*, from the mid-stage, and in *S. scrofa* at the late-stage, the ethmoturbinal I pars posterior divided from the ventral side of the ethmoturbinal I pars anterior (Fig. 6F-4, G-4, H-4, J-4). In *E. caballus*, the ethmoturbinal I pars posterior projected from the inner side of the ethmoturbinal I pars anterior, with the innermost part bifurcating (Fig. 6K-4). In *F. catus*, from the mid-stage, the ethmoturbinal I pars posterior and the ethmoturbinal I pars anterior shared a common root (Fig. 6L-4, M-4).

Other ethmoturbinals in the ethmoturbinal recesses (excluding ethmoturbinal I)

Turbinals were located in the ethmoturbinal recesses, other than ethmoturbinal I. In the foetal stage 1 of *M. pentadactyla*, the ethmoturbinal II exhibited five epiturbinals (three dorsal and two ventral) and extended straight dorsally from the inner wall of the nasal capsule toward the cavity (Fig. 3A). By foetal stage 3, the tips of the epiturbinals started to expand (Fig. 3C-5). In adults, no new epiturbinals formed, and while none of the epiturbinals split, they displayed scrolling (Fig. 3F-5). From foetal stages 1 to 4, the ethmoturbinal III projected from the inner wall toward the cavity, with a single epiturbinal protruding rostrally and dorsally (Fig. 3A–D). By foetal stage 5, the dorsal tip of the ethmoturbinal III began to expand. In adults, the innermost lamina of the ethmoturbinal III showed a double scroll outward, with one dorsal epiturbinal that bifurcated.

From foetal stages 1 to 5, the ethmoturbinal IV lacked epiturbinals, extending from the inner wall into the cavity and rostrally. Its innermost part showed some expansion (Fig. 3A-6, B-6, C-6, D-6, E-6). In adults, this innermost region exhibited a double scroll outward.

In *M. javanica*, the ethmoturbinal II was similar to that of *M. pentadactyla*, extending dorsally from the inner wall toward the cavity (Fig. 4A-5). In adults, each epiturbinal scrolled, with the innermost epiturbinal scrolling outward (Fig. 4B-5). In the late-stage foetus, the ethmoturbinal III had an expanded dorsal tip, similar to *M. pentadactyla*. In adults, the innermost lamina of the ethmoturbinal III showed a double scroll outward, forming a dorsal epiturbinal that bifurcated (Fig. 4B-5).

The late-stage foetus of *M. javanica* had no epiturbinals on ethmoturbinals IV or V (Fig. 4A-5). However, in adults, the ethmoturbinals IV and V exhibited an innermost double scroll outward (Fig. 4B-6).

In adults of species other than *S. gigantea*, the ethmoturbinal II had a structure similar to that of *M. pentadactyla* (Figs 3F-5, 5A-5, B-5, C-5, D-5, E-5). Only in *S. gigantea* did ethmoturbinal II extend toward the nasal cavity with less dorsal elongation than in other species. The number of epiturbinals on ethmoturbinal II varied, with *S. gigantea* having the most (five), each splitting (Fig. 5B-5), and *P. tricuspis* and *P. tetradactyla* having fewer (one or two ridges), which did not split (Fig. 5A-5). In *M. culionensis* and *P. tricuspis*, ethmoturbinal III had a structure similar to that of *M. pentadactyla*, where the innermost lamina scrolled outward with a dorsal epiturbinal (Fig. 5A-5). *Smutsia temminckii* lacked a dorsal epiturbinal (Fig. 5C-5), while ethmoturbinal III in *S. gigantea* showed a double scroll on its innermost lamina with four

epiturbinals (Fig. 5B-5). *Phataginus tetradactyla* also showed a double scroll on the innermost part but lacked epiturbinals (Fig. 5E-6). The ethmoturbinal IV in *P. tricuspis* showed a structure similar to that of the ethmoturbinal IV in *M. pentadactyla* (Figs 3F, 5D). In *M. culionensis*, *S. gigantea*, and *S. temminckii*, ethmoturbinal IV exhibited a double scroll on the innermost lamina, with the dorsal side scrolling significantly outward. *Smutsia gigantea* had one epiturbinal each on the dorsal and ventral sides. *Phataginus tetradactyla* lacked the ethmoturbinal IV (Fig. 5E). Ethmoturbinal V was observed in *M. culionensis* and *S. gigantea* (Fig. 5A, B). In these species, the innermost portion of the ethmoturbinal V displayed a double scroll directed outward.

In *S. murinus*, ethmoturbinal II was observed projecting ventrally from the inner wall of the nasal capsule at the early-stage (Fig. 6A-5). In the mid- and late-stages, the caudal portion curved gently outward, which in adults formed a sharp curve (Fig. 6B-5, C-5, D-5). The ethmoturbinal III appeared as a small prominence at the early-stage in *S. murinus*, with the tip expanding in the mid- and late-stages, and in adults, it bifurcated dorsally and ventrally, each side scrolling (Fig. 6A-6, B-6, C-6, D-5). In *R. leschenaultii*, ethmoturbinal II projected ventrally from the inner wall of the nasal capsule from the mid-stage onward, with a dorsal epiturbinal observed in adults but absent in foetal stages from early to late (Fig. 6F-5, G-5, H-4). Additionally, ethmoturbinal III projected dorsally from the ventral inner wall from the mid-stage, bifurcating dorsally and ventrally in adults (Fig. 6F-6, G-6, H-6).

In *S. scrofa*, ethmoturbinal II appeared at the mid-stage, projecting from the ventral inner wall of the nasal capsule, with a prominence likely representing an epiturbinal (Fig. 6I-4). In the late-stage, ethmoturbinals III and IV also projected dorsally from the ventral inner wall of the nasal capsule (Fig. 6J-6). In *E. caballus*, ethmoturbinals II, III, and IV projected from the ventral inner wall of the nasal capsule at the mid-stage, extending rostrally, with multiple epiturbinals observed on each ethmoturbinal (Fig. 6K-6). In *F. catus*, ethmoturbinal II was observed from the mid-stage on the ventral inner wall of the nasal capsule, extending dorsally with a gentle curve. From the mid-stage, a dorsal epiturbinal prominence was observed on ethmoturbinal II, and ethmoturbinal III also extended dorsally from the ventral inner wall (Fig. 6L-5, L-6). By the late-stage, the innermost tip of the ethmoturbinal III showed an expansion (Fig. 6M-6).

Interturbinal

From foetal stage 1, two interturbinals formed between ethmoturbinal I and ethmoturbinal II. These interturbinals projected from the inner wall of the nasal capsule toward the cavity, with the dorsal interturbinal extending further inward than the ventral interturbinal (Fig. 3A-5). Additionally, a single interturbinal was present between ethmoturbinal II and ethmoturbinal III, projecting from the inner wall of the nasal capsule toward the cavity and extending dorsally (Fig. 3A). From foetal stage 5, protrusions that would become interturbinals were observed between ethmoturbinal III and ethmoturbinal IV, as well as posterior to ethmoturbinal IV (Fig. 3A–E). In adults, the two interturbinals between ethmoturbinal I and ethmoturbinal II showed further development: the dorsal interturbinal scrolled dorsally and laterally, forming a branch with a double scroll on the ventral side. The ventral interturbinal was shorter than the dorsal one and displayed a double scroll (Fig. 3F-5).

The single interturbinal between ethmoturbinal II and ethmoturbinal III divided rostrocaudally, scrolling outward with a double scroll. The interturbinals between ethmoturbinal III and ethmoturbinal, IV and posterior to ethmoturbinal IV, remained as small protrusions (Fig. 3F).

In the late-stage foetus of *M. javanica*, single interturbinal protrusions were observed between ethmoturbinal I and ethmoturbinal II, between ethmoturbinal II and ethmoturbinal III, and between ethmoturbinal III and ethmoturbinal IV, each projecting from the inner wall toward the cavity (Fig. 4A). In the adult, the interturbinal observed between ethmoturbinal III and ethmoturbinal IV in the late-stage foetus had disappeared. This structure may have either developed into an epiturbinal-like structure or disappeared entirely without further development as an independent interturbinal (Fig. 4B, B-5). Precise identification of interturbinates and epiturbinals will require examination of specimens from post-natal growth stages, as well as the foetal period. A small interturbinal was observed posterior to ethmoturbinal IV.

For all interturbinals in adult species other than *M. pentadactyla* and *M. javanica*, which were examined in foetal stages, identifications remain provisional (Fig. 5A–E). Species showing a similar pattern to *M. pentadactyla*, with two interturbinals between ethmoturbinal I and ethmoturbinal II, included *S. gigantea*, *S. temminckii*, and *P. tricuspis* (Figs 3F-5, 5B-5, D-4). In *S. gigantea*, of the two interturbinals between ethmoturbinal I and ethmoturbinal II, the dorsal interturbinal scrolled ventrally and exhibited splitting dorsally and ventrally. The ventral interturbinal scrolled ventrally. Additionally, there were two interturbinals between ethmoturbinal II and ethmoturbinal III (Fig. 5B-5), one between ethmoturbinal III and ethmoturbinal IV, and one between ethmoturbinal IV and ethmoturbinal V. These interturbinals split rostrocaudally, with a double scroll outward (Fig. 5B). In *S. temminckii*, of the two interturbinals between ethmoturbinal I and ethmoturbinal II, the ventral interturbinal was fused with ethmoturbinal II, potentially representing an epiturbinal of ethmoturbinal II (Fig. 5C-4, C-5). Additionally, a single interturbinal was observed between ethmoturbinal II and ethmoturbinal III (Fig. 5C-5).

In *P. tricuspis*, the dorsal interturbinal between ethmoturbinal I and ethmoturbinal II divided dorsoventrally, forming a double scroll outward (Fig. 5D-4). The ventral interturbinal was shorter and also split dorsoventrally (Fig. 5D-5). The interturbinals between ethmoturbinal II and ethmoturbinal III, as well as between ethmoturbinal III and ethmoturbinal IV, were only slightly protruding (Fig. 5D). *Manis culionensis* and *P. tetradactyla* each had a single interturbinal between ethmoturbinal I and ethmoturbinal II, which divided dorsoventrally and formed a double scroll outward (Fig. 5A-5, E-5). Compared to other species, *M. culionensis* and *P. tetradactyla* exhibited an exceptionally low number of interturbinals. Their interturbinals may have fused with the ethmoturbinals, possibly appearing as epiturbinals due to their close association.

In *S. murinus*, from the mid-stage onward, an interturbinal was observed protruding as a ridge from the inner wall of the nasal capsule between ethmoturbinal I and ethmoturbinal II (Fig. 6B-5,

C-5, D-5). In adults, this interturbinal bifurcated into inner and outer branches, with the inner branch scrolling strongly ventrally (Fig. 6D-5). In *R. leschenaultii*, no interturbinal was observed during the early- and mid-stages. From the late-stage onward, an interturbinal was present, protruding from the nasal capsule between tethmoturbinal I and ethmoturbinal II (Fig. 6G-5, H-5). In *S. scrofa*, a single interturbinal was observed from the late-stage, protruding between ethmoturbinal I and ethmoturbinal II (Fig. 6J-5). In *E. caballus*, at the mid-stage, a single interturbinal was observed between ethmoturbinal I and ethmoturbinal II, between ethmoturbinal II and ethmoturbinal III, between ethmoturbinal III and ethmoturbinal IV, and between ethmoturbinal IV and ethmoturbinal V (Fig. 6K). Notably, the rostral interturbinals located between ethmoturbinal I and ethmoturbinal II, as well as between ethmoturbinal II and ethmoturbinal III, exhibited multiple splitting (Fig. 6K-5). In *F. catus*, a single interturbinal was observed protruding between ethmoturbinal I and ethmoturbinal II from the mid-stage (Fig. 6L-5, M-5).

DISCUSSION

Research on the nasal turbinals of pholidotans is limited, although numerous studies have examined their morphology. Studies have primarily focused on the Asian genus *Manis*, particularly *M. javanica*. Detailed morphology of nasal turbinals have been described in adults (Weber 1891, 1904, Martinez *et al.* 2024b), neonates (Jollie 1968), and foetuses (Weber 1891, Starck 1941). However, research has predominantly concentrated on *M. javanica*, with few studies on other species. Parker (1885) only mentioned the nasoturbinal and maxilloturbinal of *M. pentadactyla*. Wright *et al.* (2024) reconstructed the turbinals of *M. culionensis* using a μCT scanner. Fewer studies have been conducted on the African lineages of pholidotans, such as *Smutsia* and *Phataginus*, compared to the genus *Manis*. Research has been conducted on adult *P. tetradactyla* (Wiedemann, 1907) and foetal *S. temminckii* (Parker 1885). These studies only illustrate certain turbinals but do not identify or provide detailed descriptions of individual nasal turbinals. Recent studies have reconstructed the nasal turbinals and laminae of *P. tetradactyla* (Wright *et al.* 2024) and *S. gigantea* (Martinez *et al.* 2024b, Wright *et al.* 2024) in three dimensions, providing detailed structural descriptions. Furthermore, the specimens used in the studies by Rapp (1852), Parker (1885), and Negus (1958) did not specify the exact species, leaving it unclear whether the observed specimens indeed belonged to the genus *Manis*.

Weber (1891) presented the first comprehensive study on the morphology of nasal turbinals in pholidotans, using adult and foetal *M. javanica* specimens collected from Sumatra and Java. In his study, he examined the turbinals through sagittal sections and published schematic figures showing cross-sections of the nasal cavity, viewed internally with the nasal septum removed. While he observed foetal turbinals in a similar sagittal view as the adult specimens, he only examined a portion of the turbinals in the foetus. Additionally, studies on species belonging to the genus *Manis* include investigations of an *M. pentadactyla* foetus (Parker 1885), *M. javanica* foetuses (Weber 1891, Starck 1941), and neonates (Jollie 1968). Parker (1885) did not examine cross-sections of the nasal cavity in the *M. pentadactyla* foetus but briefly mentioned specific turbinal structures without providing detailed identification of the nasal turbinals. Starck (1941) conducted the most detailed study on the nasal turbinals of an *M. javanica* foetus, although the locality of the specimen used in his study is unknown. In his work, he presented several coronal sections of the nasal cavity. Jollie (1968) provided detailed coronal sections of the nasal cavity of neonatal *M. javanica* specimens collected from Java, describing their turbinal morphology. These studies revealed both consistencies and discrepancies in the identification of turbinals in *M. javanica*. These inconsistencies may be due to differences in the developmental stages of the specimens examined. Weber (1891) studied adults, Starck (1941) examined foetuses, and Jollie (1968) observed neonates. Moreover, differences in the sections examined may also be a contributing factor. Indeed, Weber (1891) examined sagittal sections, while Starck (1941) and Jollie (1968) used coronal sections.

While there is agreement among these studies, their results differ from our identification of the turbinals. Specifically, what Weber (1891), Starck (1941), and Jollie (1968) identified as ethmoturbinal I and ethmoturbinal II in the ethmoturbinal recess of *M. javanica*, we consider to be the ethmoturbinal I pars anterior and posterior laminae, respectively, of ethmoturbinal I. This conclusion is based on our observations of turbinal development in late-stage foetuses and adults of *M. javanica*, as well as in foetuses at multiple stages of *M. pentadactyla*, a closely related species (Figs 3, 4). In *M. pentadactyla*, the ethmoturbinal I splits from the earliest foetal stage (Fig. 3A), and the first and second ethmoturbinals in the rostral region of *M. javanica* foetuses resemble the structures of ethmoturbinal I pars anterior and pars posterior in the largest *M. pentadactyla* foetuses (Figs 3, 4). The most rostral ethmoturbinal, which we identified as ethmoturbinal I pars anterior in both *M. pentadactyla* and *M. javanica*, corresponds to the ethmoturbinal I structure described by Weber (1891) in adult *M. javanica*, by Starck (1941) in foetuses, and by Jollie (1968) in neonates (Figs 3, 4). The first ethmoturbinal in the rostral region of *M. javanica* (previously identified as ethmoturbinal I, but identified herein as ethmoturbinal I pars anterior) and the second ethmoturbinal (previously identified as ethmoturbinal II, but identified herein ethmoturbinal I pars posterior) have their roots in contact but do not share the same root (Fig. 4). In some individuals, depending on their locality, the roots of the first and second ethmoturbinals are separated (Martinez *et al.* 2024b). Starck (1941) and Jollie (1968) considered the first and second ethmoturbinals in the rostral region to be separate ethmoturbinals. Weber (1891, 1904) identified them without observing the structure of their roots, as his observations were made from sagittal sections. The dividing of ethmoturbinal I (into pars anterior and pars posterior) is a structure commonly observed in mammals, including those within laurasiatherians (Fig. 6) (Allen 1882, Martinez *et al.* 2024a, b, Wright *et al.* 2024). This supports the hypothesis that the first and second ethmoturbinals in the rostral region of *M. javanica* are both part of ethmoturbinal I.

The difference in the identification of the turbinal is primarily due to observational or interpretational variations in the root of the distinct lamella. Additionally, it is influenced by how terminology is applied to each structure. For example, in rodents, Ruf (2020) considered ethmoturbinal I to be divided into a pars

anterior and a pars posterior, whereas Smith and Bonar (2022) identified them as ethmoturbinals I and II. Even among studies on *M. javanica*, there are differences in the terminology used. Weber (1891) adopted terminology that does not divide ethmoturbinal I, as used by Zuckerkandl (1887). In contrast, although Starck (1941) did not explicitly describe it, he used the terminology employed by Voit (1909) and Peter (1912), while Jollie (1968) followed the terminology used by Reinbach (1952a, b, 1955). In these terminologies, ethmoturbinal I is divided into pars anterior and pars posterior. Future work will need to address this question at the placental scale (see also: Smith and Rossie 2008).

Discrepancies in the reported number of ethmoturbinals were observed not only among previous studies, but also when compared with our observations. These differences are probably not merely due to confusion of the laminae of ethmoturbinal I (pars anterior and pars posterior) but may involve more complex factors. Weber (1891) observed the turbinal of adult *M. javanica* in sagittal sections and identified seven turbinals within the ethmoturbinal recess; when using the terminology adopted by Voit (1909), the number of turbinals is counted as five (Supporting Information, Fig. S3). These observations were not conducted in coronal sections. Additionally, although *M. javanica* foetuses were examined, the use of only sagittal sections may have posed some limitations in fully capturing the intricate details of the nasal structures.

By comparing Weber's sagittal observations of the nasal cavity with our three-dimensional reconstructions based on segmentation of each turbinal in *M. javanica*, we concluded that the structures Weber identified as '4. medialer Riechwulst' in his terminology are most likely caudal lamina of ethmoturbinal I pars posterior (Fig. 4; Supporting Information, Fig. S3). Furthermore, Weber's '5. medialer Riechwulst' corresponds to what we identified as ethmoturbinal II, while his '6. medialer Riechwulst' corresponds to our ethmoturbinals III and IV. Lastly, his '7. medialer Riechwulst' aligns with what we identified as ethmoturbinal V (Fig. 4B; Supporting Information, Fig. S3).

While Weber's observation of both foetal and adult specimens was a suitable approach for identifying turbinals and laminae, his method of identifying turbinals based solely on a single sagittal section, rather than using multiple coronal sections, has limited a more comprehensive identification of turbinals. In foetuses, after the ethmoturbinals have protruded into the nasal capsule, epiturbinals emerge from each ethmoturbinal, while interturbinals tend to protrude from the inner wall of the nasal capsule, as well as from each turbinal (Peter 1912). Observing from a single sagittal section does not allow for accurate identification of whether the nasal turbinals are ethmoturbinals, interturbinals, or epiturbinals splitting from the ethmoturbinals. Therefore, an observation method that accurately captures the protrusion from the inner wall of the nasal capsule, as well as from each turbinal, is crucial for improving identification (Feng *et al.* 2022).

In Jollie's study (1968) of a neonatal *M. javanica*, he reported the presence of seven ethmoturbinals, which exceeds the number reported by Weber (1891). Jollie (1968) probably considered some of the rostral ethmoturbinals as separate entities and interpreted interturbinals as ethmoturbinals, leading to the higher count. The structure Jollie (1968) identified as ethmoturbinal III in coronal sections resembles what we identified as the caudal interturbinal of ethmoturbinal II in both *M. pentadactyla* and *M. javanica*. Furthermore, the turbinal that Jollie (1968) labelled as ethmoturbinal VII in his three-dimensional reconstruction of the nasal capsule does not extend inward in adults, suggesting that it is, in fact, an interturbinal (Fig. 4B-5).

Starck (1941), in his observations of *M. javanica* foetuses, reported five ethmoturbinals within the ethmoturbinal recess. He questioned the excessively high number of ethmoturbinals reported in Weber's observations of an adult. Since Starck (1941) did not examine adults, he could not conclude the final number of ethmoturbinals in *M. javanica*, considering the possibility that the number might increase during the transition from foetal to adult. In this study, we compared foetal specimens at a developmental stage similar to those observed by Starck (1941) with adult specimens. We confirmed that only epiturbinals arise from the ethmoturbinals, and the number of ethmoturbinals themselves does not increase (Fig. 4). The pronounced discrepancy in the number of ethmoturbinals reported by Starck (1941) and Weber (1891) can be attributed chiefly to differences in the terminology each author employed. Starck (1941) followed the nomenclature of Voit (1909) and Peter (1912), who subdivided ethmoturbinal I when identifying individual elements. By contrast, Weber (1891) stated that he drew on Zuckerkandl's terminology (1887), yet the terms he actually used were not identical; for example, like Paulli (1900a,b,c), he designated the lsc as the first and most rostral turbinal (Supporting Information, Fig. S3).

A common challenge encountered by both Starck (1941) and Jollie (1968), who observed less complex nasal turbinals in foetuses and neonates using coronal sections, was identifying the first and second ethmoturbinals in the rostral region as ethmoturbinals I and II. In fact, what they identified as ethmoturbinals I and II were laminae of ethmoturbinal I. This interpretation probably arose from the unique structure of *M. javanica*, where ethmoturbinal I becomes divided and appears as two separate, independent ethmoturbinals. In the closely related species *M. pentadactyla*, the most rostral ethmoturbinal I is large and subdivides into pars anterior and pars posterior, a configuration consistent with the ethmoturbinal I structure in other mammals (Figs 3, 5) (Allen 1882, Reinbach 1952a, b).

Frontoturbinal recess

In both *M. pentadactyla* and *M. javanica*, the frontoturbinal protrudes from the inner wall of the nasal capsule, a feature also observed in other laurasiatherians. Comparative studies between pholidotans and armadillos were conducted by Reinbach (1952b), who proposed an armadillo *bauplan* based on observations of armadillo foetuses (Reinbach 1952a). In his work, Reinbach (1952b) described the presence of a septum within the frontoturbinal recess, referred to as frontoturbinal septum, a structure characteristic of Xenarthra. He concluded that the septum frontoturbinal is a synapomorphic trait of xenarthrans. At the same time, Reinbach (1952b) noted that pholidotans lack the septum frontoturbinal in the frontoturbinal recess and suggested that this absence is an apomorphic trait. Since molecular phylogenetic studies have confirmed that pholidotans belong to Laurasiatheria (Shoshani *et al.* 1985, Murphy *et al.* 2001a, b, Meredith

et al. 2011, O'Leary *et al.* 2013), we propose that the absence of the septum frontoturbinal in pholidotans represents a synapomorphic trait of boreoeutherians. This structure is also absent in other laurasiatherians (Fig. 6) and in euarchontoglirans, including rodents (Ruf 2004), rabbits (Ruf 2014), scandentians (Ruf *et al.* 2015, Feng *et al.* 2022), and primates (Smith and Rossie 2008, Smith *et al.* 2011, 2016, Maier and Ruf 2014, Wagner *et al.* 2024).

Maxilloturbinal

Rapp (1852) indicated that the maxilloturbinal bends only ventrally, though the species he observed could not be identified. Herein, we report contrasting observations. In Asian pholidotans of the genus *Manis*, the maxilloturbinal branches into two, with only *M. culionensis* exhibiting a small caudal projection in the maxilloturbinal. In contrast, African pholidotans of the genera *Smutsia* and *Phataginus* exhibit a distinct three-way branching pattern, with two branches at the rostral side and a third dorsal branch at the caudal end. Weber (1891, 1904) noted that in *M. javanica*, the maxilloturbinal decreases in size toward the caudal end, though this pattern appears characteristic of the Asian lineage. In the African lineage, the caudal part of the maxilloturbinal appears to retain a more substantial size, potentially due to the presence of branching. These findings indicate possible variations in maxilloturbinal morphology between pholidotan lineages, warranting further investigation.

Nasoturbinal and lamina semicircularis

In pholidotans, the nasoturbinal and lamina semicircularis are fused together, a structure observed in all laurasiatherians except for pteropodids, which lack the nasoturbinal (Figs 3–6) (Ito *et al.* 2021, 2022). In eulipotyphlans, the nasoturbinal and lamina semicircularis develop separately (Ito *et al.* 2022); however, their developmental patterns remain unknown in other taxa. Research on eulipotyphlans has demonstrated that the nasoturbinal and lamina semicircularis develop separately (Ito *et al.* 2022). In early-stage *M. pentadactyla* foetuses, the nasoturbinal and lamina semicircularis are fused, making it difficult to determine whether they develop separately in pholidotans. Additionally, a clear boundary at the junction between the nasoturbinal and lamina semicircularis is difficult to identify. Identifying the precise junction between the nasoturbinal and lamina semicircularis is challenging in foetal pholidotans. Additionally, while the nasoturbinal is typically considered a structure that fuses with the nasal bone (Negus 1958), observations of pholidotan development suggest that the nasoturbinal arises from two distinct structures: one originating from the nasal capsule and the other from the nasal bone.

Turbinals and laminae evolution

The bony structures forming the nasal turbinals are extremely thin and fragile, making it rare for fossils to preserve their detailed features. In the absence of key fossils that could inform the study of turbinal evolution at the common ancestor of pholidotans, inferences based on extant species and recent phylogenetic trees are necessary (Maier 1983, Maier and Ruf 2014, Ruf *et al.* 2014, 2021).

Summarizing the common structures of the turbinals and laminae in species belonging to the pangolin family, the nasoturbinal is positioned dorsally within the nasal cavity and extends longitudinally from the rostral to the caudal direction. The lamina semicircularis bridges the dorsal and ventral parts of the nasal cavity, while the lamina horizontalis spreads horizontally, dividing the nasal cavity into dorsal and ventral sections (Figs 3–5). The structures of the lamina semicircularis and lamina horizontalis in pholidotans do not show significant differences when compared to those in other laurasiatherians (Fig. 5) or euarchontoglirans. This suggests that the nasoturbinal, lamina semicircularis, and lamina horizontalis of the common ancestor of pholidotans must be similar to those of extant pholidotans.

Regarding the structure of the maxilloturbinal, the maxilloturbinals in *M. pentadactyla* and *M. javanica* show double-scrolled folds (Figs 3, 4). In *Smutsia* and *Phataginus*, the folds are also double-scrolled but have an additional caudal branch (Fig. 5B–E). *Manis culionensis*, although smaller than these two genera, has a slight branch on the caudal side (Fig. 5A).

In other laurasiatherians, the structure of the maxilloturbinal varies within Eulipotyphla, with species such as moles and soricids having double-scrolled folds, while species like hedgehogs exhibit branched maxilloturbinals (Ito *et al.* 2022). In carnivorans, species with both double-scrolled folds and branched maxilloturbinals are also found within this clade. Additionally, in perissodactylans and cetartiodactylans, many species show maxilloturbinals with double-scrolled folds. In *S. scrofa* and *Bison*, the maxilloturbinal has two main branches, with additional branches further diverging from these (Zuckerkandl 1887, Negus 1958). In *E. caballus*, the maxilloturbinal does not have large branches but instead forms a dorsal scroll shape (Negus 1958, Kupke *et al.* 2016). In chiropterans, pteropodoids are considered to have an ancestral turbinal morphology, characterized by a branched maxilloturbinal (Ito *et al.* 2021).

Given this diversity, it remains unclear whether the common ancestor of laurasiatherians had a double-scrolled or branched maxilloturbinal, and it is similarly uncertain whether the common ancestor of pholidotans had a double-scrolled or branched maxilloturbinal. However, it is unlikely that the common ancestor of pholidotans had an extensively branched maxilloturbinal, as seen in some carnivoran species. The evolutionary scenario of the maxilloturbinal in Pholidota can be considered as follows. In the common ancestor of Pholidota, the maxilloturbinal had a double-scroll structure and a branched morphology on the caudal side. Subsequently, it is hypothesized that this caudal branching structure disappeared or was reduced in the Asian lineage.

In pholidotans, variation in the number of frontoturbinals is observed, with species having between three and five (Table 1). Eulipotyphlans typically have two frontoturbinals (Fig. 6A–D; Table 2) (Pauli 1900c, Woehrmann-Repenning and Meinel 1977, Ito *et al.* 2022). Perissodactylans and cetartiodactylans tend to have a higher number of frontoturbinals (Fig. 6I–K; Table 2) (Paulli 1990b, c). Among carnivorans, many species have more than three frontoturbinals, with canids typically having three and ursids having four (Paulli 1990c). Based on these observations, it is likely that the number of frontoturbinals increased in the common ancestor of perissodactylans, cetartiodactylans, carnivorans, and pholidotans. From these observations, we can infer that the common ancestor of pholidotans probably had three or more frontoturbinals (Fig. 7).

In mammals, ethmoturbinal I generally divides into pars anterior and pars posterior, as observed in boreoeutherians (Figs 3–6; Tables 1, 2) (Ruf 2004, 2014, Smith and Rossie 2008, Smith *et al.* 2011, Maier and Ruf 2014, Ruf *et al.* 2015, Feng *et al.* 2022) and Afrotheria (Stößel *et al.* 2010). This structure is also present in *M. pentadactyla* and *S. gigantea*. In *M. culionensis*, however, the ethmoturbinal I pars anterior and pars posterior are completely separated, appearing as independent ethmoturbinates. This separation of pars anterior and pars posterior in *M. culionensis* is more pronounced than in *S. temminckii*, *P. tricuspis*, and *P. tetradactyla*. In *M. javanica*, the roots of pars anterior and pars posterior of the ethmoturbinal I are in contact (Figs 3F-4, 5A-4, B-4, C-4; Table 1).

From this, two possible scenarios can be considered for the evolution of ethmoturbinal I in pholidotans. In Scenario 1, the pars anterior and pars posterior of ethmoturbinal I became completely separated in some species. This scenario is the most likely. The reasoning is that the morphology of ethmoturbinals II and III in late-stage foetuses of *M. pentadactyla* and *M. javanica* are similar, and in adult *M. javanica*, the structure of ethmoturbinal I pars posterior is similar to the ethmoturbinal structures located posterior to ethmoturbinal I in *M. culionensis*, *S. temminckii*, *P. tricuspis*, and *P. tetradactyla*. In the common ancestor of pholidotans, as in other mammals, ethmoturbinal I consisted of pars anterior and pars posterior. In *M. culionensis*, *S. temminckii*, and the common ancestor of *P. tricuspis* and *P. tetradactyla*, the pars anterior and pars posterior of ethmoturbinal I may have become completely divided, giving the appearance of independent turbinals (Fig. 7).

In Scenario 2, the common ancestor of pholidotans, as in other mammals, had an ethmoturbinal I with pars anterior and pars posterior. In *M. culionensis* and in the common ancestor of *S. gigantea*, *S. temminckii*, *P. tricuspis*, and P. tetradactyla; however, the pars anterior and pars posterior became completely separated. Subsequently, in *S. gigantea*, the previously separated pars anterior and pars posterior fused again (Fig. 7). Under this scenario, the structures of ethmoturbinal I in *M. pentadactyla* and *S. gigantea* would not resemble each other, and their developmental patterns would probably differ. However, based on our observations of adults, the ethmoturbinal I morphology of these two species appears quite similar. Since the development of *S. gigantea* was not observed in this study, we cannot fully assess the validity of Scenario 2 (Fig. 7).

Finally, we discuss the evolution of the number of ethmoturbinals. In cetartiodactylans, species of *Bos* have four ethmoturbinals, while species of *Sus* have six (Paulli 1900b). In perissodactylans, *E. caballus* has five ethmoturbinals, and *Tapirus* has six (Paulli 1900b). Among carnivorans, *Canis* (Paulli 1990c, Wagner and Ruf 2021), *Felis* (Paulli 1990c), and *Ursus* (Paulli 1990c) have three ethmoturbinals, whereas *Nasua* has five (Paulli 1990c) (Table 2). Based on the number of ethmoturbinals observed in the pangolin species examined in this study, it is likely that the common ancestor of cetartiodactylans, perissodactylans, carnivorans, and pholidotans had at least three ethmoturbinals. For the common ancestor of pholidotans, the number of ethmoturbinals is estimated to have been four (Fig. 7). In evolutionary Scenarios 1 and 2 for ethmoturbinal I, it is inferred that one ethmoturbinal was gained in the common ancestor of *M. javanica*, *M. culionensis*, and *S. gigantea*, while one ethmoturbinal was lost in *P. tetradactyla* (Fig. 7).

A functional perspective

The elongated snout and specialized diet of pholidotans have been hypothesized to be linked to larger olfactory turbinals, a pattern that has been demonstrated in one group of highly specialized worm-eating rodents, where larger olfactory turbinals are thought to be associated with higher olfactory sensitivity (Martinez *et al.* 2018, 2024a, c). However, quantitative comparisons of olfactory turbinals between pholidotans and certain Carnivora do not support this hypothesis for this clade (Wright *et al.* 2024). Genomic data also do not provide strong support, as pholidotans possess between 444 and 1066 functional olfactory receptor genes, a range comparable to that of Carnivora (Han *et al.* 2022). Nevertheless, olfactory capabilities and the complex relationship between anatomical and genomic proxies remain debated topics requiring further research (Bird *et al.* 2018, Christmas *et al.* 2023, Martinez *et al.* 2023b, 2024c). The diceCT data provided by this study offer the opportunity for future research to quantitatively assess epithelial surface area, rather than depending solely on bony proxies.

CONCLUSION

Using DiceCT imaging, we three-dimensionally reconstructed and observed the development of the nasal capsule in five prenatal stages of *M. pentadactyla* and in prenatal stages of *M. javanica*. Based on these observations, we examined adult specimens from seven of the eight extant pangolin species. While this provided valuable comparative insights, accurate identification of the turbinals and laminae would ideally require observations across developmental series, from foetal to adult, in all eight species. Despite this limitation, our analysis allowed us to clarify the homology of the turbinals and laminae in this group. By mapping the turbinals and laminae characteristics observed in our study on to a phylogenetic tree, we proposed an evolutionary scenario for turbinals and laminae within pholidotans.

Pholidotans are characterized by possessing the long nasoturbinal that extends in the rostrocaudal direction and the lamina semicircularis that expands medially, features shared with other Boreoeutherians. Regarding the structure of the maxilloturbinals, *Manis* exhibits double-scrolled folds, while *Smutsia* and *Phataginus* have a double-scrolled structure with a small caudal branch, indicating structural differences between the Asian and African lineages. Furthermore, the number of frontoturbinals varies between three and five. Variation is also observed in the turbinals within the ethmoturbinal recess across pangolin species.

In *M. pentadactyla* and *S. gigantea*, the pars anterior and pars posterior of ethmoturbinal I share the same root. In *M. javanica*, there is variation among individuals: in some, the roots of ethmoturbinal I pars anterior and pars posterior are in contact, while in others, these roots are completely separated. In *M. culionensis*, *S. temminckii*, *P. tricuspis*, and *P. tetradactyla*, ethmoturbinal I pars anterior and pars posterior are entirely separated.

Based on these observations, we propose two evolutionary scenarios for the ethmoturbinals. In both scenarios, ethmoturbinal I in the common ancestor of pholidotans is interpreted as a

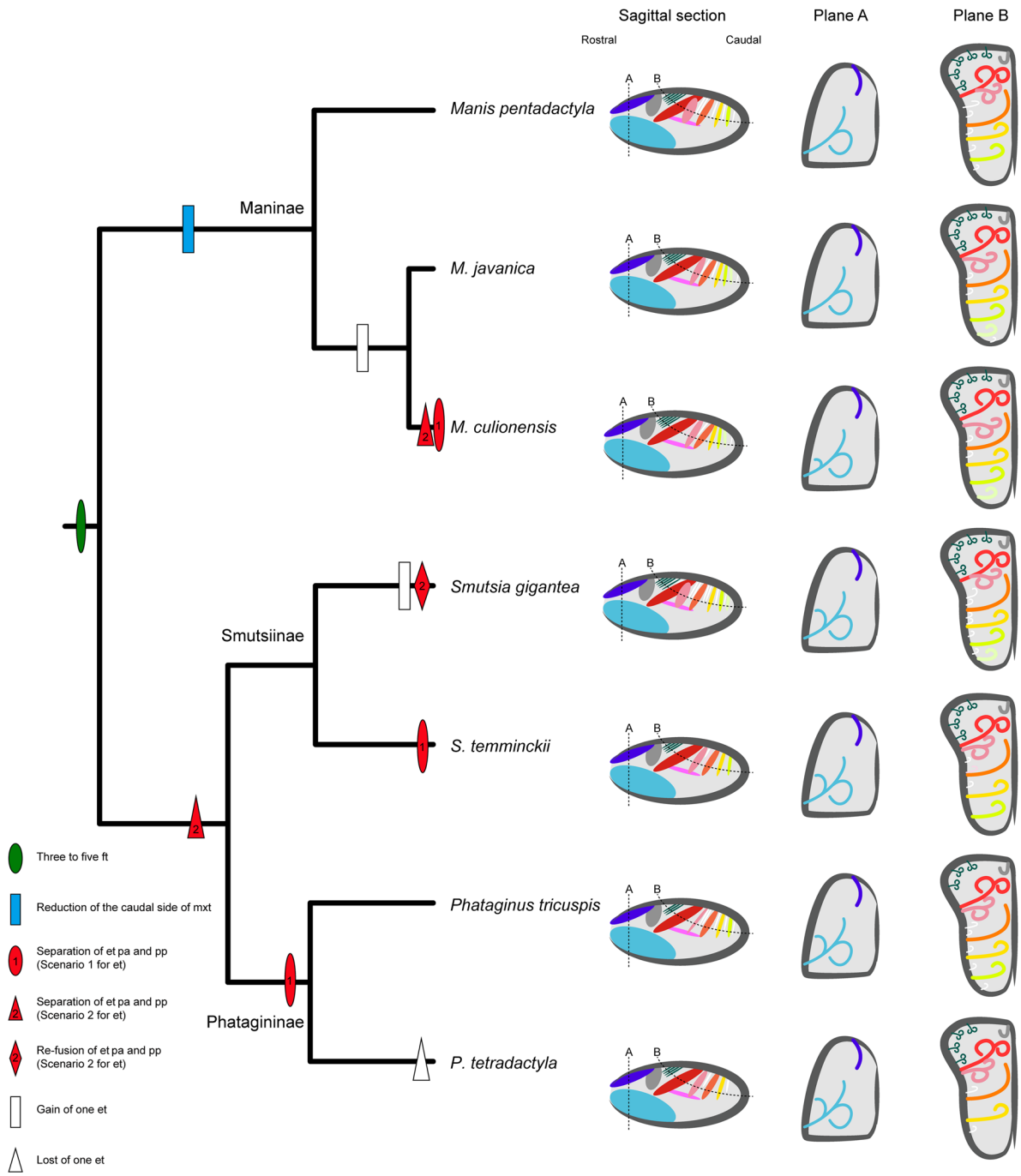

Figure 7. Inferred evolutionary history of the nasal structures. nasoturbinal (purple); maxilloturbinal (light blue); frontoturbinal (green, light green); lamina semicircularis (grey); lamina horizontalis (pink); ethmoturbinal I pars anterior (red); ethmoturbinal I pars posterior (light coral); ethmoturbinal II (orange); ethmoturbinal III (yellow); ethmoturbinal IV (light yellow); interturbinal (white); uncertain (cherry pink).

plesiomorphic structure, consisting of distinct pars anterior and pars posterior, as seen in typical boreoeutherians. Scenario 1 suggests that in *M. culionensis*, *S. temminckii*, and the common ancestor of *P. tricuspis* and *P. tetradactyla*, ethmoturbinal I became fully separated, resulting in the appearance of two distinct ethmoturbinals. Scenario 2 proposes that ethmoturbinal I became fully separated in *M. culionensis* and the common ancestor of *S. gigantea*, *S. temminckii*, *P. tricuspis*, and *P. tetradactyla*, and later re-fused in *S. gigantea*. To further deepen our understanding of the evolution of turbinals and laminae in pholidotans, it is essential to accurately determine the homology of these structures. Observations of the growth process of turbinals from foetuses and newborns to adults are required.

ACKNOWLEDGEMENTS

We would like to express our sincere gratitude to Professor W. Maier, whose profound insights into anatomical evolution and development greatly influenced our research of nasal structures. We also thank Dr D. Koyabu and Dr L.A.B. Wilson for organizing

the discussion sessions that helped advance this study. We are deeply indebted to Dr I. Ruf and Dr I. Werneburg for their assistance in examining older literature sources. We further extend our appreciation to Dr F. Meguro, Dr K. Koyasu, Dr M. Oishi, and Dr T. Nojiri for their support in managing and transporting the outgroup mammalian fetal specimens. We gratefully acknowledge Dr D.E. Winkler, Dr M. Ishikawa, and Dr T. Kubo for their valuable technical and academic advice. We are also thankful to Dr L. Hautier for generously sharing CT data. We also thank Dr G. Ferreira for his logistical support with data that will be used for other research articles. In addition, we extend our sincere appreciation to Dr S. Kawada at the National Museum of Nature and Science (Kahaku), who facilitated the use of the museum's foetal specimens for this study, and to Dr S. Merker for granting access to the mammal collections at the Stuttgart Museum of Natural History (SMNS).

SUPPLEMENTARY DATA

Supplementary data is available at *Zoological Journal of the Linnean Society* online.

CONFLICT OF INTEREST

None declared.

FUNDING

This research was supported by the Alexander von Humboldt Foundation (Q.M. FRA-1222365-HFST-P.) to Q.M., the Bundesministerium für Bildung und Forschung (BMBF; Project KI-Morph 05D2022) to Q.M., and the Japan Society for the Promotion of Science (JSPS KAKENHI 22J40028, 23K14248) to K.I.

DATA AVAILABILITY

The data underlying this article are not publicly available because of museum collection policy, but are available from the corresponding author on reasonable request.

REFERENCES

Allen H. On a revision of the ethmoid bone in the Mammalia, with special reference to the description of this bone and of the sense of smelling in the Cheiroptera. *Bulletin of the Museum of Comparative Zoology* 1882;**10**:135–71.

de Beer GR. The development of the skull of the shrew. *Philosophical Transactions of the Royal Society of London B* 1929;**217**:411–80.

de Beer GR. *The Development of the Vertebrate Skull*. Oxford: Clarendon Press, 1937.

Bird DJ, Murphy WJ, Fox-Rosales L *et al.* Olfaction written in bone: cribriform plate size parallels olfactory receptor gene repertoires in Mammalia. *Proceedings of the Royal Society B: Biological Sciences* 2018;**285**:20180100.

Cave AJ, Haines RW. The paranasal sinuses of the anthropoid apes. *Journal of Anatomy* 1940;**74**:493–523.

Cuvier G. *Tableau Élémentaire de l'Histoire Naturelle des Animaux*. Paris: Baudouin, 1798.

Christmas MJ, Kaplow IM, Genereux DP; Zoonomia Consortium§ *et al.* Evolutionary constraint and innovation across hundreds of placental mammals. *Science* 2023;**380**:eabn3943.

Dieulafe L, Loeb HW. Morphology and embryology of the nasal fossae of vertebrates. *Annals of Otology, Rhinology & Laryngology* 1906;**15**:1–60.

Fawcett E. The primordial cranium of *Erinaceus europaeus*. *Journal of Anatomy* 1918;**52**:211–50.45. (pagination in source may vary; original article "Pt 2," p. 211).

Feng Y, Xia W, Zhao P *et al.* Survey anatomy and histological observation of the nasal cavity of *Tupaia belangeri chinensis* (Tupaiidae, Scandentia, Mammalia). *The Anatomical Record* 2022;**305**:1448–58.

Ganeshina LV, Vorontsov NN, Chabovsky VI. Comparative morphological study of the nasal cavity structure in certain representatives of the order Insectivora. *Zoologicheskii Zhurnal* 1957;**36**:122–38.

Gaubert P, Antunes A, Meng H *et al.* The complete phylogeny of pangolins: scaling up resources for the molecular tracing of the most trafficked mammals on Earth. *The Journal of Heredity* 2018;**109**:347–59.

Gaudin TJ, Wible JR. The entotympanic of pangolins and the phylogeny of the Pholidota (Mammalia). *Journal of Mammalian Evolution* 1999;**6**:39–65.

Gaudin TJ, Emry RJ, Wible JR. The phylogeny of living and extinct pangolins (Mammalia, Pholidota) and associated taxa: a morphology based analysis. *Journal of Mammalian Evolution* 2009;**16**:235–305.

Giannini NP, Macrini TE, Wible JR *et al.* The internal nasal skeleton of the bat *Pteropus lylei* K. Andersen, 1908 (Chiroptera: Pteropodidae). *Annals of Carnegie Museum* 2012;**81**:1–17.

Gignac PM, Kley NJ. Iodine-enhanced micro-CT imaging: methodological refinements for the study of the soft-tissue anatomy of post-embryonic vertebrates. *Journal of Experimental Zoology. Part B, Molecular and Developmental Evolution* 2014;**322**:166–76.

Gignac PM, Kley NJ, Clarke JA *et al.* Diffusible iodine-based contrast-enhanced computed tomography (diceCT): an emerging tool for rapid, high-resolution, 3-D imaging of metazoan soft tissues. *Journal of Anatomy* 2016;**228**:889–909.

Göbbel L. The external nasal cartilages in Chiroptera: significance for intraordinal relationships. *Journal of Mammalian Evolution* 2000;**7**:167–201.

Green PA, Valkenburgh B, Pang B *et al.* Respiratory and olfactory turbinal size in canid and arctoid carnivorans. *Journal of Anatomy* 2012;**221**:609–21.

Gu T, Wu H, Yang F *et al.* Genomic analysis reveals a cryptic pangolin species. *Proceedings of the National Academy of Sciences of the United States of America* 2023;**120**:e2304096120.

Gurtovoi NN. Ecological-morphological differences in the structure of the nasal cavity in the representatives of the orders Insectivora, Chiroptera, and Rodentia. *Zoologicheskii Zhurnal* 1966;**45**:1536–51.

Han W, Wu Y, Zeng L *et al.* Building the Chordata Olfactory Receptor Database using more than 400,000 receptors annotated by Genome2OR. *Science China. Life Sciences* 2022;**65**:2539–51.

Hillenius WJ. The evolution of nasal turbinates and mammalian endothermy. *Paleobiology* 1992;**18**:17–29.

Ioana AN. Etude comparative des cornets nasaux chez: *Talpa europaea* L., et *Neomys fodiens* Schreb. (Ord, Insectivora) de Roumanie. *Travaux du Museum d'Histoire Naturelle 'Grigore Antipa'* 1970;**10**:359–63.

Ito K, Tu VT, Eiting TP *et al.* On the embryonic development of the nasal turbinals and their homology in bats. *Frontiers in Cell and Developmental Biology* 2021;**9**:613545–19.

Ito K, Kodeara R, Koyasu K *et al.* The development of nasal turbinal morphology of moles and shrews. *Vertebrate Zoology* 2022;**72**:857–81.

Jollie M. The head skeleton of a new-born *Manis javanica* with comments on the ontogeny and phylogeny of the mammal head skeleton. *Acta Zoologica* 1968;**49**:227–305.

Kaucka M, Petersen J, Tesarova M *et al.* Signals from the brain and olfactory epithelium control shaping of the mammalian nasal capsule cartilage. *eLife* 2018;**7**:1–27.

Kupke A, Wenisch S, Failing K *et al.* Intranasal location and immunohistochemical characterization of the equine olfactory epithelium. *Frontiers in Neuroanatomy* 2016;**10**:97.

Kuramoto K, Nishida T, Mochizuki K. Morphological studies on the nasal turbinals of the musk shrew. *Nihon Juigaku Zasshi. The Japanese Journal of Veterinary Science* 1980;**42**:377–80.

Larochelle R, Baron G. Comparative morphology and morphometry of the nasal fossae of four species of North American shrews (*Soricinae*). *The American Journal of Anatomy* 1989;**186**:306–14.
Linnaeus C. *Systema Naturae per Regna Tria Naturae Secundum Classes, Ordines, Genera, Species, Cum Characteribus, Differentiis, Synonymis, Locis*, 10th edn. Stockholm: Laurentii Salvii, 1758.
Macrini TE. Comparative morphology of the internal nasal skeleton of adult marsupials based on X-ray computed tomography. *Bulletin of the American Museum of Natural History* 2012;**365**:1–91.
Macrini TE. Development of the ethmoid in *Caluromys philander* (Didelphidae, Marsupialia) with a discussion on the homology of the turbinal elements in marsupials. *Anatomical Record (Hoboken, NJ: 2007)* 2014;**297**:2007–17.
Maier W. Nasal structures in Old and New World primates. In: RL Ciochon, AB Chiarelli (eds), *Evolutionary Biology of the New World Monkeys and Continental Drift*. New York: Springer, 1980, 219–241.
Maier W. Morphology of the interorbital region of *Saimiri sciureus*. *Folia Primatologica; International Journal of Primatology* 1983;**41**:277–303.
Maier W. Cranial morphology of the therian common ancestor, as suggested by the adaptations of neonate marsupials. In: FS Szalay, MJ Novacek, MC McKenna (eds), *Mammal Phylogeny*. New York: Springer, 1993a, 165–81.
Maier W. Zur evolutiven und funktionellen Morphologie des Gesichtsschädels der Primaten. *Zeitschrift für Morphologie und Anthropologie* 1993b;**79**:279–99.
Maier W. Ontogeny of the nasal capsule in cercopithecoids: a contribution to the comparative and evolutionary morphology of catarrhines. In: PF Whitehead, CJ Jolly (eds), *Old World Monkeys*. Cambridge: Cambridge University Press, 2000, 99–132.
Maier W. A neglected part of the mammalian skull: the outer nasal cartilages as progressive remnants of the chondrocranium. *Vertebrate Zoology* 2020;**70**:367–82.
Maier W, Ruf I. Morphology of the nasal capsule of Primates—with special reference to *Daubentonia* and *Homo*. *The Anatomical Record* 2014;**297**:1985–2006.
Martineau-Doizé B, Caya I, Martineau G-P. Osteogenesis and growth of the nasal ventral conchae of the piglet. *Journal of Comparative Pathology* 1992;**106**:323–31.
Martinez Q, Lebrun R, Achmadi AS *et al.* Convergent evolution of an extreme dietary specialisation, the olfactory system of worm-eating rodents. *Scientific Reports* 2018;**8**:17806–13. https://doi.org/10.1038/s41598-018-35827-0
Martinez Q, Clavel J, Esselstyn JA *et al.* Convergent evolution of olfactory and thermoregulatory capacities in small amphibious mammals. *Proceedings of the National Academy of Sciences of the United States of America* 2020;**117**:8958–65. https://doi.org/10.1073/pnas.1917836117
Martinez Q, Okrouhlík J, Šumbera R *et al.* Mammalian maxilloturbinal evolution does not reflect thermal biology. *Nature Communications* 2023a;**14**:4425. https://doi.org/10.1038/s41467-023-39994-1
Martinez Q, Courcelle M, Douzery E *et al.* When morphology does not fit the genomes: the case of rodent olfaction. *Biology Letters* 2023b;**19**:20230080. https://doi.org/10.1098/rsbl.2023.0080
Martinez Q, Amson E, Ruf I *et al.* Turbinal bones are still one of the last frontiers of the tetrapod skull: hypotheses, challenges and perspectives. *Biological Reviews* 2024a. https://doi.org/10.1111/brv.13122
Martinez Q, Wright M, Dubourguier B, *et al.* Disparity of turbinal bones in placental mammals. *The Anatomical Record* 2024b, 1–29. https://doi.org/10.1002/ar.25552
Martinez Q, Amson E, Laska M. Does the number of functional olfactory receptor genes predict olfactory sensitivity and discrimination performance in mammals? *Journal of Evolutionary Biology* 2024c;**37**:238–47. https://doi.org/10.1093/jeb/voae006
Meredith RW, Janečka JE, Gatesy J *et al.* Impacts of the Cretaceous Terrestrial Revolution and KPg extinction on mammal diversification. *Science (New York, N.Y.)* 2011;**334**:521–4.
Michelsson G. Das Chondrocranium des Igels (*Erinaceus europaeus*). *Zeitschrift für Anatomie und Entwicklungsgeschichte* 1922;**65**:509–43.
Moore WJ. *The Mammalian Skull*. Cambridge: Cambridge University Press, 1981.
Murphy WJ, Eizirik E, O'Brien SJ *et al.* Resolution of the early placental mammal radiation using Bayesian phylogenetics. *Science (New York, N.Y.)* 2001;**294**:2348–51.
Murphy WJ, Eizirik E, Johnson WE *et al.* Molecular phylogenetics and the origins of placental mammals. *Nature* 2001;**409**:614–8.
Negus V. *Comparative Anatomy and Physiology of the Nose and Paranasal Sinuses*. Edinburgh: Livingstone, 1958.
O'Leary MA, Bloch JI, Flynn JJ *et al.* The placental mammal ancestor and the post–K-Pg radiation of placentals. *Science* 2013;**339**:662–7.
Parker WK. On the structure and development of the skull in the Mammalia. *Philosophical Transactions of the Royal Society of London* (various parts), 1885.
Parker WK. On the structure and development of the skull in the pig (*Sus scrofa*). *Philosophical Transactions of the Royal Society of London* 1874;**164**:289–336.
Paulli S. Über die Pneumaticität des Schädels bei den Säugetieren. Eine morphologische Studie. I. Über den Bau des Siebbeins. *Gegenbaurs Morphologisches Jahrbuch* 1900a;**28**:147–78.
Paulli S. Über die Pneumaticität des Schädels bei den Säugetieren. Eine morphologische Studie. II. Über die Morphologie des Siebbeins und die Pneumaticität bei den Ungulaten und den Proboscisden. *Gegenbaurs Morphologisches Jahrbuch* 1900b;**28**:179–251.
Paulli S. Über die Pneumaticität des Schädels bei den Säugetieren. Eine morphologische Studie. III. Über die Morphologie des Siebbeins und die der Pneumaticität bei den Insectivoren, Hyracoideen, Chiropteren, Carnivoren, Pinnipedien, Edentaten, Rodentiern, Prosimiae. *Gegenbaurs Morphologisches Jahrbuch* 1900c;**28**:483–564.
Peter K. Die Entwicklung der Nasenmuscheln bei Mensch und Säugetieren. *Archiv für Mikroskopische Anatomie* 1912;**80**:478–559.
Rapp WV. *Anatomische Untersuchungen über die Edentaten*. Tübingen: Laupp'schen Buchhandlung, 1852.
Reinbach W. Zur Entwicklung des Primordialcraniums von *Dasypus novemcinctus* Linné (*Tatusia novemcincta* Lesson). I. *Zeitschrift für Morphologie und. Anthropologie* 1952a;**44**:375–444.
Reinbach W. Zur Entwicklung des Primordialcraniums von *Dasypus novemcinctus* Linné (*Tatusia novemcincta* Lesson). II. *Zeitschrift für. Morphologie Und Anthropologie* 1952b;**45**:1–72.
Reinbach W. Das Cranium eines Embryos des Gürteltieres *Zaedyus minutus* (65 mm Sch.-St). *Morphologisches Jahrbuch* 1955;**95**:79–141.
Rossie JB. Ontogeny and homology of the paranasal sinuses in Platyrrhini (Mammalia: Primates). *Journal of Morphology* 2006;**267**:1–40.
Roux GH. The cranial development of certain Ethiopian 'insectivores' and its bearing on the mutual affinities of the group. *Acta Zoologica* 1947;**28**:165–397.
Rowe TB, Eiting TP, Macrini TE *et al.* Organization of the olfactory and respiratory skeleton in the nose of the gray short-tailed opossum *Monodelphis domestica*. *Journal of Mammalian Evolution* 2005;**12**:303–36.
Ruf I. Vergleichend-ontogenetische Untersuchungen an der Ethmoidalregion der Muroidea (Rodentia, Mammalia). Ph.D. Thesis, Universität Tübingen, 2004.
Ruf I. Comparative anatomy and systematic implications of the turbinal skeleton in Lagomorpha (Mammalia). *Anatomical Record (Hoboken, NJ: 2007)* 2014;**297**:2031–46.
Ruf I. Ontogenetic transformations of the ethmoidal region in Muroidea (Rodentia, Mammalia): new insights from perinatal stages. *Vertebrate Zoology* 2020;**70**:383–415.
Ruf I, Maier W, Rodrigues PG *et al.* Nasal anatomy of the non-mammaliaform cynodont *Brasilitherium riograndensis* (Eucynodontia, Therapsida) reveals new insight into mammalian evolution. *Anatomical Record (Hoboken, N.J.: 2007)* 2014;**297**:2018–30.
Ruf I, Janßen S, Zeller U. The ethmoidal region of the skull of *Ptilocercus lowii* (Ptilocercidae, Scandentia, Mammalia)—a contribution to the reconstruction of the cranial morphotype of primates. *Primate Biology* 2015;**2**:89–110.
Ruf I, Meng J, Fostowicz-Frelik Ł. Anatomy of the nasal and auditory regions of the fossil lagomorph *Palaeolagus haydeni*: systematic and evolutionary implications. *Frontiers in Ecology and Evolution* 2021;**9**:636110.

Schmidt U, Nadolski A. Die Verteilung von olfaktorischem und respiratorischem Epithel in der Nasenhöhle der Hausspitzmaus, *Crocidura russula* (Soricidae). *Zeitschrift für Säugetierkunde* 1979;**44**:18–25.
Sharma DR. Studies on the anatomy of the Indian insectivore, *Suncus murinus*. *Journal of Morphology* 1958;**102**:427–553.
Shoshani J, Goodman M, Czelusniak J, Braunitzer G. A phylogeny of Rodentia and other Eutherian orders: parsimony analysis utilizing amino acid sequences of alpha and beta hemoglobin chains. In: WP Luckett, J-L Hartenberger (eds), *Evolutionary Relationships among Rodents*. New York: Springer, 1985, 191–210.
Smith TD, Bonar CJ. The nasal cavity in agoutis (*Dasyprocta* spp.): a micro-computed tomographic and histological study. *Vertebrate Zoology* 2022;**72**:95–113.
Smith TD, Rossie J. Primate olfaction: anatomy and evolution. In: W Brewer, D Castle, C Pantelis (eds), *Olfaction and the Brain: Window to the Mind*. Cambridge: Cambridge University Press, 2006, 135–66.
Smith TD, Rossie JB. Nasal fossa of mouse and dwarf lemurs (Primates, Cheirogaleidae). *Anatomical Record (Hoboken, N.J.: 2007)* 2008;**291**:895–915.
Smith TD, Rossie JB, Bhatnagar KP. Evolution of the nose and nasal skeleton in primates. *Evolutionary Anthropology: Issues, News, and Reviews* 2007;**16**:132–46.
Smith TD, Eiting TP, Rossie JB. Distribution of olfactory and nonolfactory surface area in the nasal fossa of *Microcebus murinus*: implications for microcomputed tomography and airflow studies. *Anatomical Record (Hoboken, NJ: 2007)* 2011;**294**:1217–25.
Smith TD, Eiting TP, Bhatnagar KP. Anatomy of the nasal passages in mammals. In: RL Doty (ed.), *Handbook of Olfaction and Gustation*, 3rd edn. Hoboken: John Wiley & Sons, 2015, 37–62.
Smith TD, Martell MC, Rossie JB *et al.* Ontogeny and microanatomy of the nasal turbinals in Lemuriformes. *Anatomical Record* 2016;**299**:1492–510. https://doi.org/10.1002/ar.23465
Smith TD, Curtis A, Bhatnagar KP *et al.* Fissures, folds, and scrolls: the ontogenetic basis for complexity of the nasal cavity in a fruit bat (*Rousettus leschenaultii*). *Anatomical Record (Hoboken, NJ: 2007)* 2021a;**304**:883–900.
Smith TD, DeLeon VB, Eiting TP *et al.* Venous networks in the upper airways of bats: a histological and diceCT study. *Anatomical Record* 2021b;**304**:1–21.
Söllner B, Kraft R. Anatomie und Histologie der Nasenhöhle der Europäischen Wasserspitzmaus, *Neomys fodiens* (Pennant 1771), und anderer mitteleuropäischer Soriciden (Insectivora, Mammalia). *Spixiana* 1980;**3**:251–72.
Starck D. Zur Morphologie des Primordialcraniums von *Manis javanica* Desm. *Gegenbaurs Morphologisches Jahrbuch* 1941;**86**:1–122.
Storr GKC. *Prodromus Methodi Mammalium*. Tübingen: Literis Erhardianis, 1780.
Stößel A, Junold A, Fischer MS. The morphology of the eutherian ethmoidal region and its implications for higher-order phylogeny. *Journal of Zoological Systematics and Evolutionary Research* 2010;**48**:167–80.
Van Gilse PHG. The development of the sphenoidal sinus in man and its homology in mammals. *Journal of Anatomy* 1927;**61**:153–66.
Van Valkenburgh B, Theodor J, Friscia A *et al.* Respiratory turbinates of canids and felids: a quantitative comparison. *Journal of Zoology* 2004;**264**:281–93.
Van Valkenburgh B, Curtis A, Samuels JX *et al.* Aquatic adaptations in the nose of carnivorans: evidence from the turbinates. *Journal of Anatomy* 2011;**218**:298–310.
Van Valkenburgh B, Pang B, Bird D *et al.* Respiratory and olfactory turbinals in feliform and caniform carnivorans: the influence of snout length. *Anatomical Record* 2014;**297**:2065–79.
Van Valkenburgh B, Smith TD, Craven BA. Tour of a labyrinth: exploring the vertebrate nose. *Anatomical Record (Hoboken, N.J.: 2007)* 2014;**297**:1975–84.
Vicq-d'Azyr F. *Encyclopédie Méthodique. Système Anatomique*. Paris: Agasse, 1792.
Voit M. Das Primordialcranium des Kaninchens–unter Berücksichtigung der Deckknochen. *Beiträge und Referate zur Anatomie und Entwickelungsgeschichte* 1909;**38**:425–616. (exact pagination per part may vary).
Wagner F, Ruf I. 'Forever young'—postnatal growth inhibition of the turbinal skeleton in brachycephalic dog breeds (*Canis lupus familiaris*). *Anatomical Record (Hoboken, NJ: 2007)* 2021;**304**:154–89.
Wagner F, DeLeon VB, Bonar CJ *et al.* How the youngsters teach the 'old timers': terminology of turbinals in adult primates inferred from ontogenetic stages. *Vertebrate Zoology* 2024;**74**:487–509. https://doi.org/10.3897/vz.74.e126944
Weber M. *Beiträge zur Anatomie und Entwickelung des Genus Manis*. Jena: Gustav Fischer, 1891.
Weber M. *Die Säugetiere. Einführung in die Anatomie und Systematik der recenten und fossilen Mammalia*. Jena: Gustav Fischer, 1904.
Wible JR. On the cranial osteology of the Hispaniolan solenodon, *Solenodon paradoxus* Brandt, 1833 (Mammalia, Lipotyphla, Solenodontidae). *Annals of Carnegie Museum* 2008;**77**:321–402.
Wiedersheim R. *Einführung in die Vergleichende Anatomie der Wirbeltiere*. Jena: Gustav Fischer, 1907.
Wilson DE, Mittermeier RA. *Handbook of the Mammals of the World. Vol. 2: Hoofed Mammals*. Barcelona: Lynx Edicions, 2011.
Woehrmann-Repenning A, Meinel W. A comparative study on the nasal fossae of *Tupaia glis* and four insectivores. *Anatomischer Anzeiger* 1977;**142**:331–45.
Wright M, Martinez Q, Cardoso SF *et al.* Sniffing out morphological convergence in the turbinal complex of myrmecophagous placentals. *The Anatomical Record* 2024, 1–27. https://doi.org/10.1002/ar.25603
Youssef EH. The chondrocranium of *Hemiechinus auritus aegyptius* and its comparison with *Erinaceus europaeus*. *Acta Anatomica* 1971;**78**:224–54.
Zeller U. Morphogenesis of the mammalian skull with special reference to *Tupaia*. *Mammalia Depicta* 1987;**13**:17–50.
Zhang F, Wu S, Zou C *et al.* A note on captive breeding and reproductive parameters of the Chinese pangolin, *Manis pentadactyla* Linnaeus, 1758. *ZooKeys* 2016;**618**:129–44.
Zuckerkandl E. *Das Periphere Geruchsorgan der Säugethiere: Eine Vergleichend-Anatomische Studie*. Wien: Wilhelm Braumüller, 1887.